# RADIATIVE DECAYS OF LIGHT MESONS*

By M. Zieliński

Institute of Computer Science, Jagellonian University, Cracow**

I review present experimental and theoretical status of electromagnetic decays of light mesons. Special attention is paid to single-photon decays of charged resonances, and to recent applications of the Primakoff technique to measure such processes. New data on radiative decays of pseudoscalar, vector, axial and tensor mesons are compared with several theoretical calculations involving quark models, unitary symmetry relations, and an effective Lagrangian approach. Vector Meson Dominance ideas, as applied to meson spectroscopy, are discussed in detail. Also, the electromagnetic properties of the $A_1$ meson are examined in the context of resonance parameters observed in diffractive production and $\tau$-lepton decays. Finally, I emphasize the importance of radiative processes in searching for glueball and hybrid states of matter.

PACS numbers: 13.40. Hg, 13.60. Le, 14.40. Cs, 14.80. Pb

## 1. Introduction

One of the major trends in particle physics has been the exploration of ever deeper levels of substructure of matter. Photons, both virtual and real, their interactions theoretically well understood, provide particularly clean probes of properties of complex objects. Scattering of light, and the inverse process of light emission, has proved to be an invaluable tool of research in condensed matter, atomic, and nuclear physics. The same appears to hold true in the field of elementary particles. Hard interactions of virtual photons in deep inelastic lepton scattering have led to an understanding of the short distance structure of nucleons. Soft interactions of photons with hadrons are sensitive to larger-scale properties of hadron wave functions, and such information is usually less ambiguous than that from investigations using purely hadronic processes. Electromagnetic decays of mesons, in particular, have been recognized for some time as important for gaining an understanding of the large-distance structure of elementary particles.

Lacking a fundamental dynamical theory of hadrons, a rich phenomenology has been developed over the years to deal with electromagnetic properties of mesons; some of the

---

popular approaches have involved quark model [1], unitary symmetries [2, 3] and the vector meson dominance hypothesis [4, 5]. On the experimental side, there has been great activity in the measurement of radiative decay widths. Progress in the field of electromagnetic properties of mesons has been particularly impressive. In this review I discuss new information on radiative decays of light mesons (i.e. mesons not containing charmed, or heavier, quarks), and its impact on the understanding of structure and couplings of hadrons involved in such decays. Many of the underlying ideas are relatively old, and by now fairly standard. I will therefore briefly introduce the more successful formulations used in the past, and relate them to the more recent approaches.

Stimulated by the accuracy of the new data, and developments within QCD that have been applied to hadron spectroscopy through, e.g., QCD sum rules [6], QCD bag models [7] and potential approaches [8, 9], recent theoretical examinations of meson radiative decays have concentrated on more global tests and extensions of the previous work. In the course of the following discussion I compare the latest data with several recent calculations to evaluate the success of different approaches and to establish the level of model dependence of the predictions. Particular attention is paid to single-photon decays of mesons and their phenomenological consequences. Henceforth, throughout the paper, the term "radiative decays" refers specifically to single-photon transitions.

Most of the new experimental results on radiative decays have been obtained using the Primakoff technique, which, at high energies, emerges as a major tool for such measurements (for two-photon decays a similar role is played by studies of photon-photon collisions in the $e^+e^-$ interactions). Consequently, I present in some detail the basics of the Primakoff method, discuss specific requirements posed for experiments, describe an example experimental setup (the E272 at Fermilab), and evaluate the inherent accuracy of this method (Section 2).

In Section 3, I review the new data and several theoretical calculations of electromagnetic decays of vector and pseudoscalar mesons. In particular, various alternatives to nonrelativistic quark-model calculations, developed to explain an apparent suppression of the decay rates, are discussed. In Section 4, the experimental and theoretical status of electromagnetic decays of axial and tensor mesons is presented. Special attention is paid to the still controversial $A_1$ meson. Proper evaluation of the experimental situation on its radiative properties required a somewhat detailed examination of diffractive-production and $\tau$-lepton decay data relevant to this meson.

In Section 5, I discuss the role that electromagnetic transitions play in searches for expected novel states of hadronic matter, such as QCD glueballs and hybrid mesons. The electromagnetic decays of such candidate states can place valuable constraints on their interpretations. The viability of the Primakoff method as a technique of searching for hybrid mesons is emphasized. Section 6 is devoted to a summary and a general outlook on the direction of this field of research.

The issues discussed in this paper cover a rather specialized area of research on electromagnetic properties of mesons. The selection of topics was dictated by the author's interests and by his involvement in some of the original research (mostly experimental). Recent presentations of related material can be found in several excellent reviews that provide

overviews of: the physics of two-photon collisions [10], electromagnetic transition form-factors for mesons [11], earlier work on meson radiative decays [12, 13], and radiative decays of mesons containing heavy quarks [14, 15].

## 2. Methods used for radiative width measurements

### 2.1. An overview of methods

With notable exceptions of $\pi^0 \to \gamma\gamma$, $\eta \to \gamma\gamma$, $\omega \to \pi^0\gamma$ and $\eta' \to \varrho^0\gamma$ transitions, electromagnetic decays of mesons comprise small fractions (of order of $10^{-3} - 10^{-4}$) of all available channels. Clean observation of a radiative decay requires therefore that there be no large background contributions to the final state of interest. Serious backgrounds can occur, however, even in the case of exclusive production channels. For example, the direct measurement of the $\varrho^+ \to \pi^+\gamma$ decay width is not feasible, because the $\varrho^+$ branching into $\pi^+\gamma$ is only 0.046%, and backgrounds from $\varrho^+ \to \pi^+\pi^0 \to \pi^+\gamma\gamma$ decays, where one soft photon is not detected, exceed the size of the signal. This problem is encountered in cases where there exists a matching hadronic decay mode with the photon substituted by the $\pi^0$, and it is additionally aggrevated if the full width of the decaying hadron is large (the $K^{*+} \to K^+\gamma$ decay is another example).

As a consequence of the above, only a limited number of radiative widths could have been measured through direct observation of the relevant final states. I will now briefly summarize the methods that have been successful in direct determinations of the radiative widths of several mesons.

1. The most direct technique involves measuring the decay length of a particle. This was used recently in an elegant and accurate determination of the $\pi^0 \to \gamma\gamma$ decay [16]. The experiment took advantage of the relatively long mean decay length of high energy $\pi^0$ mesons produced in the interactions of 450 GeV protons. The $\pi^0$'s were observed by detecting 150 GeV positrons produced by the $\pi^0$-decay $\gamma$-rays converting in a target consisting of two thin tungsten foils. The variation of the conversion rate $Y(d)$ with the foil separation $d$ was measured over the range of 5–250 μm. $Y(d)$ is related to the $\pi^0$ decay length $\lambda$ through a slightly modified decay-in-flight distribution:

$$Y(d) \propto A + B(1 - \exp(-d/\lambda)),$$

where the constant term $A$ has been introduced to account for the yield of positrons that did not depend on foil separation (e.g., due to promptly produced positrons and $\gamma$-rays, or photons from $\eta$ decays). The above distribution was convoluted with the momentum distribution of pions, as determined from charged pions produced in the same experiment. The $\pi^0$ lifetime has been found to be $\tau_{\pi^0} = (0.867 \pm 0.022 \pm 0.017) \times 10^{-16}$ sec.

2. The charge exchange reaction

$$\pi^- p \to Mn$$
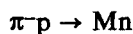
was used as a clean source of $M = \eta, \eta', \omega$ mesons that were subsequently detected in their radiative decay modes. The following relative branching ratios were determined

from such studies: $\omega \to \pi^0\gamma/\omega \to 3\pi$ [17], $\omega \to \pi^0\gamma/\omega \to$ all [18], $\omega \to \eta\gamma/\omega \to \pi^0\gamma$ [19], $\eta' \to \omega\gamma/\eta' \to \eta\pi^+\pi^-$ [20]. The corresponding radiative widths were finally extracted using the table values of known widths of the reference processes.

3. The $V \to \gamma\gamma$ radiative decays of neutral vector mesons $V = \varrho^0, \omega, \phi$ were measured in the following photoproduction process [21]

$$\gamma Cu \to VCu, \quad V \to \eta\gamma \to \gamma\gamma\gamma.$$

The absolute normalization of the decay rates was obtained from the known branching value for the decays $\omega \to \pi^0\gamma$, which were also registered in the experiment. The result for the $\phi \to \eta\gamma$ decay width agreed well with $e^+e^-$ storage ring determinations (see below). However, two solutions were obtained for the $\varrho^0$ and $\omega$ decay widths into $\eta\gamma$, each with different values of $\varrho^0 - \omega$ interference phase ($\approx 0°$ or $\approx 180°$). In the following I use the solution preferred by quark-model arguments (i.e. the one with the interference phase $\approx 0°$), which is consistent with other available measurements, and fits much better into the overall pattern of radiative decays of vector and pseudoscalar mesons.

4. Resonant $e^+e^-$ annihilation provides a natural source of neutral vector mesons. It is a particularly convenient way of studying the decays of the $\phi$ meson, the hadronic production of which is subject to the OZI-rule suppression. The measurement of cross-sections for $e^+e^- \to \phi \to \eta\gamma, \pi^0\gamma$ [22] allowed determinations of the $\phi \to \eta\gamma$ and $\phi \to \pi^0\gamma$ radiative widths. The branching $\omega \to \pi^0\gamma/\omega \to 3\pi$ and upper limits on $\omega \to \eta\gamma/\omega \to \pi^0\gamma$, $\omega \to \pi^0\pi^0\gamma/\omega \to \pi^0\gamma$ were also obtained from measurements of $e^+e^-$ annihilation on resonance (last reference of [22]).

5. The two-photon widths of neutral, positive $C$-parity mesons can be determined using photon-photon scattering in inelastic $e^+e^-$ collisions [23]:

$$e^+e^- \to e^+e^-\gamma^*\gamma^* \to e^+e^-M.$$
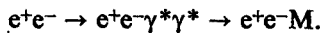
The photons that are radiated off the electron lines and collide to form the meson M are, unlike in the case of decay, slightly off-mass-shell. However, the usual imposition of tag requirements (keeping the scattering angles of the electrons very small) selects events with the invariant masses of the colliding virtual photons close to zero, so that the assumption of equality of the production and decay couplings can be justified (without electron tagging large-angle scattering corrections are necessary for proper interpretation of the results).

The cross-section for the process $e^+e^- \to e^+e^-M$ can be expressed as a convolution of the luminosities of the radiated photons, and the cross-section for the resonance production of the meson M in the interaction of two photons. Calculating the photon fluxes in the equivalent photon approximation, and assuming for simplicity a narrow total width of the M, one obtains

$$\sigma(e^+e^- \to e^+e^-M) = 64\alpha^2(2J+1)\frac{\Gamma(M \to \gamma\gamma)}{m_M^3}\ln\frac{2E}{m_M}\ln^2\frac{E}{m_e}. \quad (2.1)$$

The characteristic features of exclusive meson production in two-photon collisions can be seen in the above formula: the direct proportionality of the production cross-section to the

two-photon decay width of M, and the strong increase of $\sigma$ with collision energy. (A more detailed presentation, and a discussion of approximations involved in (2.1) can be found, e.g., in [10].)

Many two-photon decay-width measurements have been performed in the past few years, these include measurements of the $\pi^0$, $\eta$, $\eta'$, $A_2$, f, f', and $\delta(980)$ mesons; upper limits on two-photon widths of the $\iota(1460)$, $\theta(1710)$, $S*(975)$ and $\varepsilon(1300)$ have been also obtained. A detailed summary of the recent results was given, e.g., in [10]; the corresponding averages are included in Tables III and V below. Most of the measurements mentioned here are not direct, in the sense that the mesons of interest are not necessarily observed in their radiative two-photon decay mode (except in case of the $\pi^0$ and $\eta$ mesons).

6. Until recently, the most accurate determinations of the two-photon widths of the $\pi^0$ and $\eta$ mesons relied on the Primakoff technique [24], applied to coherent meson photoproduction in the Coulomb field of nuclei:

$$\gamma A \to \gamma\gamma^*A \to MA, \quad M = \pi^0, \eta$$

(with the meson M observed in its two-photon decay mode) [25, 26, 27]. The Coulomb field of a nucleus is represented by an effective photon target, the properties of which are calculable using the Weizsäcker-Williams method. As previously, the equality of the two--photon formation and decay coupling constants of the M provides the means of expressing the electromagnetic production of a desired final state (two-photon systems of a specified mass) in terms of a single unknown parameter, the two-photon decay width ($\Gamma(\pi^0 \to \gamma\gamma)$ or $\Gamma(\eta \to \gamma\gamma)$ in the present case). Primakoff measurements of the $\pi^0 \to \gamma\gamma$ width [25, 26] agree with other determinations; there is, however, a disagreement between the Primakoff and the photon-photon collision results in case of the $\eta \to \gamma\gamma$ decay width. I will comment more on this point shortly.

The original suggestion of Primakoff [24] to determine the $\pi^0 \to \gamma\gamma$ width by measuring the inverse process of $\pi^0$ photoproduction in nuclear Coulomb field was extended to include other radiative transitions as well [28, 29]. It is presently the only feasible method for measuring single-photon radiative widths of charged resonances. I will now present the Primakoff formalism, and describe, as an example, some recent measurements of radiative widths of charged mesons.

## 2.2. The Primakoff technique

Let us consider the general case of coherent production of a certain final state X in the electromagnetic field of a nucleus $A$, of charge $Ze$, by an incident charged particle a:

$$aA \to a\gamma^*A \to XA. \tag{2.2}$$

(The case of an incident photon requires only a change of spin factors in the following expressions.) A full description for the production of X has to include strong production mechanisms as well. I shall consider strong-interaction background separately. Both the electromagnetic and strong processes are represented in Fig. 1.
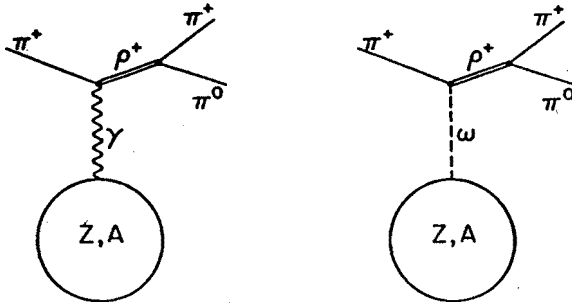
Fig. 1. Graphic representation of coherent production of the $\rho^+$ mesons on nuclei through photon and $\omega$ exchanges

The amplitude for the electromagnetic production can be calculated from the basic single-photon-exchange graph:

$$T = \langle X|j_\mu(x)|a\rangle \frac{e^2}{q^2} \langle A|j^\mu(0)|A\rangle, \qquad (2.3)$$

where $j^\mu$ is the electromagnetic current operator. At high energies and at very small momentum transfers, which are the conditions relevant to our discussion, the magnetic part of the form factor of the nucleus $A$ may be neglected. Relating the electromagnetic transition a → X to the photoproduction amplitude of X by real photons interacting with particle a, one can express the cross-section for reaction (2.2) in the following form [28]:

$$\frac{d\sigma}{dtdm^2} = \frac{Z^2\alpha}{\pi} \frac{\sigma_\gamma(m^2)}{m^2-m_a^2} \frac{t-t_{min}}{t^2} |F_{em}(t)|^2, \qquad (2.4)$$

where $m$ is the mass of the produced system, $t = |(p_X-p_a)^2|$ is the 4-momentum transfer squared (taken here as a positive quantity for convenience), and $t_{min}$ is the minimal value of $t$ allowed by kinematics, $t_{min} \approx (m^2-m_a^2)^2/4E^2$, $E$ being the energy of a in the laboratory frame. The vanishing of the production cross-section in forward direction proportionally to $(t-t_{min})$ (or to the square of the scattering angle, for small angles) follows directly from the conservation of the electromagnetic current [28]. Under the kinematic conditions of interest, only transverse photons contribute significantly to the process and, as a consequence, the helicities of incident meson a and produced system X must differ by unity.

For X being a decay product of an intermediate resonance a*, of spin $J_*$ and mass $m_*$, the photoproduction cross-section $\sigma_\gamma(m^2)$ can be related to the a* → a$\gamma$ decay width, again using the equality of the production and decay coupling constants. Taking into account different spin and phase space factors, this relation becomes:

$$\sigma_\gamma(m^2) = \frac{\pi^2}{k^2} \frac{2J_*+1}{2J_a+1} \Gamma(a^* \to a\gamma)B(a^* \to X)D(m), \qquad (2.5)$$

where $k$ is the momentum of a in the a* frame, $k = (m^2-m_a^2)/2m$, $B$ represents the branching fraction for a* → X, $J_a$ is the spin of the beam particle a, and $D(m)$ is the Breit-Wigner

distribution, normalized such that

$$D(m^2) = \frac{2}{\pi} \frac{m_*^2 \Gamma_*}{(m^2 - m_*^2)^2 + m_*^2 \Gamma_*^2} \to \delta(m - m_*) \quad \text{for} \quad \Gamma_* \to 0 \tag{2.6}$$

(this choice of normalization is particularly convenient when considering a narrow resonance). Putting everything together, we obtain

$$\frac{d\sigma}{dt\,dm^2}\bigg|_C \equiv |T_C|^2 = 4\pi Z^2 \alpha \, \frac{2J_* + 1}{2J_a + 1} \frac{m^2}{(m^2 - m_a^2)^3}$$

$$\times \Gamma(a^* \to a\gamma) B(a^* \to X) D(m) \frac{t - t_{\min}}{t^2} |F_{em}(t)|^2. \tag{2.7}$$

Care must be taken in calculating the electromagnetic nuclear form factor $F_{em}(t)$. In case of electron-nucleus scattering, the electromagnetic form factor is related to the nuclear density $\varrho(\vec{r})$ through

$$F_{em}(q^2) = \int d^3r \psi_f^*(\vec{r}) \varrho(\vec{r}) \psi_i(\vec{r}) = \int d^3r\, e^{i\vec{q}\cdot\vec{r}} \varrho(\vec{r}). \tag{2.8}$$

Although the process (2.2) proceeds also through photon exchange, the incoming and outgoing particles a and a* are hadrons and, unlike electrons, they are subject to multiple strong interactions and absorption when they pass through the nucleus. In addition, the phase of the production amplitude is modified by strong interactions with the nucleus and by the propagation of the charged particles a and a* in the nuclear Coulomb potential; such phase changes may be important for the interference of the electromagnetic and strong production mechanisms. Both effects can be taken into account [30] in the eikonal approximation, by using Coulomb-distorted waves, modified by absorption [31], for the incident and outgoing waves:

$$\psi_i(\vec{r}) = e^{ikz} \to \psi_i(\vec{r}) = e^{ikz} \exp\left(-\frac{A}{2}\sigma_a' \int\limits_{-\infty}^{z} \varrho(b, z')dz'\right) \exp\left(i\chi_C(b, z)\right) \tag{2.9}$$

and an analogous expression for the outgoing wave. In the above formula, $b$ is the impact parameter of the beam particle, $z$ is the coordinate along the collision axis and $\sigma_a' = \sigma_{aN}(1 - i\alpha_{aN})$, with $\sigma_{aN}$ being the a-nucleon total cross-section, and $\alpha_{aN}$ representing the ratio of imaginary to real parts of the a-nucleon strong-interaction scattering amplitude in forward direction. (Because the interactions of resonant states a* with nucleons are not well known, it is usually assumed that $\sigma_{a*}' = \sigma_a'$.)

The phase $\chi_C(b, z)$, due to traversing the Coulomb potential of the nucleus, is given by a straightforward integration

$$\chi_C(b, z) = \mp Z\alpha \int\limits_{-\infty}^{z} dz' \varphi(b, z'), \quad \varphi(\vec{r}) = \int d^3r' \frac{\varrho(\vec{r'})}{|\vec{r'} - \vec{r}|}. \tag{2.10}$$

The nuclear density distribution $\varrho(r)$ can be taken as the relevant Woods-Saxon distribution, normalized to unity. The above formulae can be manipulated to obtain a form more convenient for numerical integrations. References [32, 33] may be consulted for the technical points.

The effects of nuclear absorption on Coulomb production decrease with increasing energy. This is because the relevant momentum transfers are of order of a few $t_{min}$ (the maximum of the cross-section occurs at $t = 2t_{min}$), i.e. of order of $10^{-5}$ $GeV^2$ at energies of a few hundred GeV, so that most of the interactions occur at distances larger than nuclear size (typically, at distances of order of 60 fm at 200 GeV). The situation is quite different in the case of strong interactions, which can proceed through various Reggeon exchanges, and take place within the nucleus; consequently, nuclear absorption has the effect of reducing strong backgrounds that compete with electromagnetic processes.

The kinds of contributions from Reggeon exchanges depend, of course, on the nature of the a → a* transition in question. The G-parity conservation provides an important constraint on allowed exchanges in case of pion-initiated processes. Net isospin exchange is suppressed relative to isoscalar exchange, since, for coherent reactions, the amplitudes on protons and neutrons tend to cancel. For example, in the case of $\pi^+ \to \varrho^+$ transition, contributions from both ω and $A_2$ exchanges are possible. The nuclear target dependence of the ω-exchange contribution is expected to go as $A^{2/3}$ while that of the $A_2$ as $(A-2Z)^{2/3}$; nevertheless, isovector exchange may be important at intermediate energies [34] and, in general, cannot be neglected.

Finally, powerful constraints are imposed by angular momentum and parity conservation. In particular, for unnatural spin-parity changes in the a → a* vertex (e.g. $\pi^+ \to \varrho^+$), the cross-section must vanish in the forward direction. As a consequence, the cross-section for the strong contribution can be written as [30]:

$$\frac{d\sigma}{dtdm^2}\bigg|_s \equiv |T_s|^2 = c_s A^2 D(m) (t - t_{min}) |F_s(t)|^2. \tag{2.11}$$

The strong form factor $F_s(t)$ has to take into account the same nuclear absorption and Coulomb phase effects that were discussed above [30, 32, 33]. The coefficient $c_s$ represents the production strength on an isolated nucleon and can be, in principle, determined from ap → a*p transitions; in practice, however, $c_s$ is usually taken as a free parameter.

The complete cross-section, used to fit the experimental data, takes finally the form:

$$\frac{d\sigma}{dtdm^2} = |T_C + e^{i\phi}T_s|^2 \tag{2.12}$$

with $T_C$ and $T_s$ being the Coulomb and strong production amplitudes, as discussed above, and $\phi$ is a relative phase. In general, fits to experimental data (m and t dependent cross-sections measured on various nuclei) involve three free parameters: the radiative width $\Gamma(a^* \to a\gamma)$, $c_s$, and $\phi$. The latter two are of rather minor importance at high energies and small momentum transfers, as discussed below.

There are several important differences between the characteristic features of the Coulomb and strong production processes, as revealed by the formulae (2.7) and (2.11):

1. Both the photon and Reggeon exchange cross-sections (2.7), (2.11) vanish for exactly forward scattering. However, the maximum of the Coulomb production occurs very close to the forward direction, at $t = 2t_{min}$. The height of the Coulomb peak is proportional to $Z^2E^2$ and its width at half-height to $E^{-2}$. (The enhancement of the cross-section close to the forward direction is due to the pole in the $1/t^2$ photon propagator factor at $t = 0$.) After taking into account a realistic resolution (of order of several MeV) of the measured momentum transfers, cross-section (2.7) is expected to rise rapidly in the forward direction. On the other hand, the maximum of the Regge-exchange term (2.11) occurs at much larger momentum transfers, which are characteristic of nuclear size, $t \approx 0.08\, A^{-2/3}$ GeV$^2$ [35] (the amplitude for $\omega$-exchange in $\pi^+ \rightarrow \varrho^+$ transition, say, is proportional to the gradient of nuclear density and, consequently, the strong production takes place mostly at the rim of the nucleus). Therefore, at small momentum transfers, the strong-interaction background is suppressed, and can be separated from the electromagnetic production, taking advantage of the different form for the $t$-dependence. Sufficient $t$-resolution is required, however, of experiments that attempt such a separation.

2. The $t$-integrated Coulomb cross-section increases with energy as $\ln E$ (this is due to the energy dependence of $t_{min}$). The energy dependence of the Regge-exchange cross-section (2.11) is implicit in the coefficient $c_s$; depending on the exchange in question it decreases as $E^{-1}$ or faster (with the exception of the Pomeron-exchange diffractive contribu-
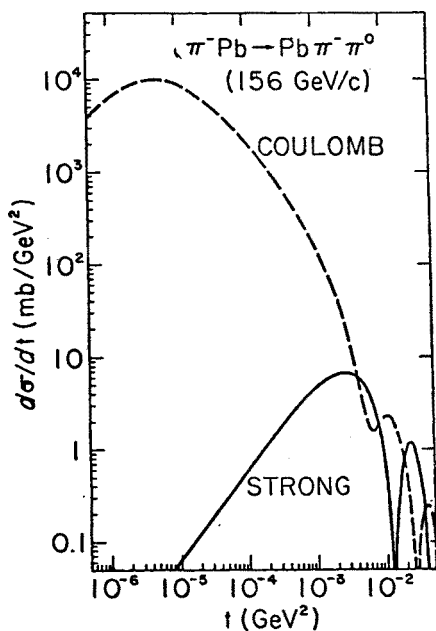


Fig. 2. Relative contributions from the Coulomb and strong terms in coherent production of the $\varrho^-$ mesons on lead at 156 GeV, prior to introduction of resolution smearing [32]

tion, which is not allowed for the transitions discussed in this paper, except for $\pi^+ \to A_1^+$).
As a consequence, at beam energies of several tens GeV or more, and $t \lesssim 0.002\ \mathrm{GeV}^2$,
the Coulomb mechanism dominates the strong contributions. The relative sizes and
$t$-dependences of the Coulomb and strong production cross-sections are illustrated in Fig. 2
for coherent $\varrho^-$ production on Pb by 156 GeV $\pi^-$ mesons.

3. The integrated Coulomb cross-section scales with the parameters of the nuclear
target as $Z^2(-1.577 - \ln bt_{\min})$, where $b$ is the effective forward slope of the form factor,
$|F(t)|^2 \simeq e^{-bt}$ and $b \approx 12A^{2/3}\ \mathrm{GeV}^{-2}$. For electromagnetic production of a state of
$m \approx 1$ GeV by a 200 GeV beam, one therefore expects $(\sigma^{\mathrm{Pb}}/\sigma^{\mathrm{Cu}})_{\mathrm{C}} \approx 6.4$. On the other
hand, the integrated hadronic cross-section (2.11) scales as $A^{2/3}$, in the absence of absorp-
tion. The absorption effects can reduce this ratio even further; their accurate estimate
requires a detailed optical-model calculation. One expects $(\sigma^{\mathrm{Pb}}/\sigma^{\mathrm{Cu}})_{\mathrm{s}} \approx 2$. The nuclear
target dependence of Coulomb production is much stronger than that of the hadronic
contribution. This feature provides an additional handle for separating the two mechanisms.

## 2.3. A Primakoff-method experiment: the E 272

The Primakoff technique provides an elegant way to study radiative transitions that
are often inaccessible to direct decay measurements. It imposes, however, specific require-
ments on experiments using this approach. As an example of an apparatus optimized for
employing the Primakoff method, I describe briefly the spectrometer of the Rochester-
-Minnesota-Fermilab collaboration. The spectrometer was used in the experiment E272
at Fermilab to collect data on transitions of beam pions and kaons to several heavier
meson states in the nuclear Coulomb field.

Experiment E272 provides a large part of the experimental material discussed in this
paper, which includes, in particular, measurements of the following coherent processes:

$$\pi^{\pm}A \to \pi^{\pm}\gamma A \qquad [36, 37] \qquad (2.13)$$

$$\pi^{\pm}A \to \pi^{\pm}\pi^0 A \qquad [32, 38, 39] \qquad (2.14)$$

$$\pi^+ A \to \pi^+\eta A \qquad [40, 41] \qquad (2.15)$$

$$\pi^+ A \to K^+ K_S^0 A \qquad [40] \qquad (2.16)$$

$$\pi^+ A \to \pi^+\pi^+\pi^- A \qquad [41, 42, 43, 44] \qquad (2.17)$$

$$\pi^+ A \to \pi^+\omega A \qquad [45] \qquad (2.18)$$

$$K^{\pm}A \to \pi^{\pm}K_S^0 A \qquad [46, 47, 48] \qquad (2.19)$$

$$K^{\pm}A \to \pi^0 K^{\pm} A \qquad [46, 47, 48] \qquad (2.20)$$

$$K^+ A \to \omega K^+ A \qquad [49] \qquad (2.21)$$

The data were taken at negative beam energies of 156 and 260 GeV and with positive
beam of 200 GeV on several targets (C, Al, Cu and Pb). Subsequent analyses of these
reactions provided measurements of the radiative widths of the $\varrho^+$, $\varrho^-$, $K^{*+}$, $K^{*-}$, $K^{**+}$,

$A_2^+$, $A_1^+$, $B^+$ mesons. The Primakoff technique has also been used in other measurements of meson radiative widths, e.g. in the determinations of the two-photon widths of the $\pi^0$ [25, 26] and $\eta$ [27] mesons. However, the E272 project was the most versatile and largest experimental program based on the Primakoff method.

The major requirements for an experiment of this kind are to obtain an accurate measurement of the very small momentum transfers involved in Coulomb production at high energies (typically of the order of several MeV), and to efficiently suppress the background interactions. Measuring the low momentum transfers requires very good
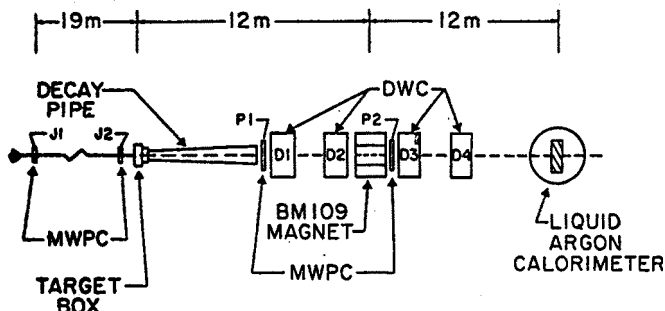


Fig. 3. Schematic diagram of the E272 spectrometer [32]

angular resolution for both charged and neutral particles. The E272 spectrometer (shown schematically in Fig. 3) was constructed to match such requirements. Since its detailed description can be found in [32, 50], I limit the presentation to recounting the features most relevant to the topics to follow.

The basic elements of the set-up consisted of 1) an evacuated target box, surrounded with veto counters used to suppress incoherent interactions and events with multiparticle production, 2) a magnetic spectrometer used to measure charged-particle trajectories and momenta, 3) a liquid argon calorimeter (LAC), used for measuring the deposition of electromagnetic energy.

The magnetic spectrometer was composed of a system of drift wire chambers (DWC), multiwire proportional chambers (MWPC) and an analysing magnet. The drift chamber system consisted of four DWC modules D1–D4, each composed of 3 pairs of chambers, rotated by different angles around the spectrometer axis, to facilitate spatial reconstruction of particle trajectories (the members of each pair were offset by ca. 1 cm to help in resolving position ambiguity). The spatial resolution of each chamber was $\approx 0.2$ mm; in effect, an average angular resolution of $\approx 0.06$ mrad was achieved for charged trajectories. The MWPC planes were used primarily for beam tagging (J1 and J2) and for triggering purposes (P1 and P2).

The magnet aperture of $0.2 \times 0.6$ m$^2$ was sufficiently large for studying relatively low--mass systems, of invariant mass $m < 1.5$ GeV. For heavier systems (especially for three charged pion final states) the acceptance was too limited to allow precision measurements. This prevented, for example, extending the range of the partial wave analysis of the data and, consequently, also of searching for exotic hybrid states (see Section 5.2) in the interest-

ing mass region above 1.5 GeV. The integrated field strength of the magnet was 3.67 Tm, corresponding to a transverse impulse of 1.1 GeV. That proved adequate for an accurate measurement of charged particle momenta over the full range. Overall momentum resolution for charged particles was $\delta p/p \approx 8 \times 10^{-5} p$ ($p$ in GeV).

Several of the final states, for which data were collected in E272, contained photons. Energies and positions of photons were measured using a finely-segmented LAC. The corresponding resolutions of the detector were determined in a calibration run using a 50 GeV electron beam. The effective energy resolution of the LAC was $\sigma^2 = 0.30 + (0.14)^2 E$, and the spatial resolution was $\approx 0.6$ mm (standard deviation per projected coordinate).

The overall momentum transfer resolution was determined largely by multiple scattering of the charged particles in the target material. To minimize this effect, only thin targets were used (a few tenths of a radiation length). Final momentum-transfer resolutions varied between 9 and 15 MeV for the studied processes. They were sufficient for a reliable separation of the Coulomb and the strong contributions.

Another important consideration for an experiment that attempts to measure such rare processes as coherent beam particle excitations in the nuclear Coulomb field is efficient rejection of other (background) interactions. The reactions of interest have typically cross-sections of order of 1 mb on a lead target, while the total $\pi^+$Pb cross-section at 200 GeV is about 2000 mb. A very selective trigger is thus a crucial requirement.

Four different trigger-logic circuits (called Rho, A1, V and Pi-E) were employed in E272 to maximize selectivity of the data taking. Their detailed definitions are beyond the purpose of this discussion, I will therefore give only a general description (more details can be found in publications on particular reactions; a comprehensive account of all E272 triggers is also given in [51]). The Rho trigger was designed to select one charged track and electromagnetic energy deposition in the LAC; reactions (2.13), (2.14), (2.20) and (2.15), with $\eta \rightarrow \gamma\gamma$, were obtained using this trigger. The A1 trigger was set up to pick out events with three charged tracks leaving the target (reactions (2.16), (2.17), (2.18), (2.19), (2.21) and (2.15) with $\eta \rightarrow 3\pi$). The V trigger selected processes in which one charged track emerged from the target and two more charged trajectories appeared downstream, the latter presumed to be decay products of a neutral long-lived particle produced at the target (reactions (2.16), (2.19), with K $\rightarrow 2\pi$). The Pi-E trigger was set up to select pion-electron scattering events.

A most important part of all triggers was suppression of incoherent interactions and multiparticle production events by veto counters surrounding the target. Judging from the quality of the data, vetoing of such background was highly effective in all cases. A contribution from incoherent production would be reflected in momentum-transfer distributions as an additional component $\exp(-bt)$, with the slope $b \approx 8$ GeV$^{-2}$, characteristic of the nucleon form factor. No such contributions were detected for any of the reactions measured in E272 (except for three charged pion production at $t > 0.5$ GeV$^2$, which is far beyond $t$-ranges relevant for Coulomb production).

The apparatus was equipped with three Cherenkov counters to determine the beam-particle type (pion, kaon or proton). There was no identification of charged particles in

the final state. In most cases this caused no problems, however, the study of coherent Kω production [49] was, to some extent, affected by the $\pi^+$ vs $K^+$ ambiguity. Also, the admixture of $K^+K^-\pi^+$ to three charged particles final states could not be separated and, consequently, all three charged particles produced by the pion beam were assumed to be pions, namely reaction (2.17). Although the kaon admixture is not expected to exceed an estimated 5%, its influence on weak partial waves, like the $1^+S1^+$ or $1^-P1^+$, was not checked (these waves, relevant for the radiative production of the $A_1$ and of a hypothetical hybrid meson, were extracted from data on three charged-particle production with signals only at the level of several percent of total intensity).

Finally, the thorough investigation of the important reference processes $K \to \pi e \nu$, $K \to 2\pi$ and $K \to 3\pi$ should be mentioned. These beam-kaon decays in flight were collected simultaneously with data on other processes, and were subsequently used to fine-tune the parameters of a Monte Carlo acceptance program for the experiment, and to determine absolute normalizations of other processes. They provided the best check on the momentum-transfer resolution of the spectrometer (for K-decays taken with no target present) and on the influence of multiple scattering in the target material (for decays taken with targets in place). The observed distributions of total energy, decay vertices, and invariant masses, agreed well with expectations based on the Monte Carlo model.

The same Monte Carlo model was also used to correct data for geometric losses of the spectrometer, inefficiencies of different parts of the apparatus, random noise effects, and inefficiencies of the event-reconstruction software. After applying corrections for all known causes of event losses, including those that were not incorporated in the Monte Carlo system (such as secondary interactions in the spectrometer material, particle decays in flight, δ-ray vetoes, etc.), the number of observed beam-K decays was somewhat smaller that expected from the known incident flux. Therefore, additional overall normalization adjustments of order of 10% (for $K \to 2\pi$) to 20% (for $K \to 3\pi$) were required to correct for event losses of unknown origin. The same corrections were also applied to other reactions of similar topology, separately for each target, beam energy, and reaction type. This procedure greatly minimized the systematic uncertainties in the experiment.

## 2.4. Tests of the Primakoff formalism

Much of recent progress in measurements of meson radiative widths has been based on the Primakoff technique. In this Section I pay special attention to tests of the formalism per se, and, in particular, to the validity of the single-photon-exchange approximation.

One of the cleanest of such tests is provided by elastic pion-photon Compton scattering in the nuclear Coulomb field. According to Eq. (2.4) the cross-section for producing a $\pi\gamma$ system in the electromagnetic field of a nucleus by an incident pion takes the form

$$\frac{d\sigma}{dt\,dm^2} = \frac{Z^2\alpha}{\pi}\frac{\sigma_{\pi\gamma}(m^2)}{m^2 - m_\pi^2}\frac{t - t_{min}}{t^2}|F_{em}(t)|^2, \tag{2.22}$$

where $m_\pi$ is the pion mass and $m$ is the mass of the $\pi\gamma$ system. The cross-section (2.22) peaks at very low values of momentum transfer, $t \approx 10^{-6}$ GeV$^2$ at the energy of 200 GeV,

which means that the exchanged photon is essentially real. Since the momentum transfer to the target is so low, the presented analysis is insensitive to nuclear form-factor effects or to the presence of any low-lying excited states of the nuclei. In the formulae below I also neglect any internal structure of the pion.

Assuming a point-like pion, the $\pi\gamma$ Compton cross-section, $\sigma_{\pi\gamma}$, is easily calculable in QED [52]. The differential Compton cross-section for unpolarized photons is

$$\frac{d\sigma_{\pi\gamma}}{d\Omega}\bigg|_{CM} = \frac{\alpha^2[(m^4+m_\pi^4)(1+\cos^2\theta)+2(m^4-m_\pi^4)\cos\theta]}{m^2[m^2+m_\pi^2+(m^2-m_\pi^2)\cos\theta]^2}, \tag{2.23}$$

which yields after integration over angles

$$\sigma_{\pi\gamma}(m^2) = \frac{4\alpha^2\pi(m^2+m_\pi^2)}{m^2(m^2-m_\pi^2)}\left[m^4-m_\pi^4+2m^2m_\pi^2\ln\left(\frac{m_\pi^2}{m^2}\right)\right] \tag{2.24}$$

($\theta$ is the scattering angle of the pion in the Gottfried-Jackson frame for $\pi\gamma$ systems). This theoretical prediction is compared below with the cross-sections measured [37] from reaction (2.13) on Cu and Pb targets at 200 GeV. Note that the following comparison does not involve any free parameters.

The $\pi^+\gamma$ mass distributions [37] are compared in Fig. 4a with theoretical predictions that have been corrected for the acceptance of the experiment. The agreement is very good. The geometric acceptance was determined using a Monte Carlo model of the spectrometer; it is shown as a function of $m$ at the top of the figure. The angular distributions of pions in the Gottfried-Jackson-frame, shown in Fig. 4b, are consistent with the simplest prediction for a point-like pion. At this level of statistics, there is no indication of pion-structure effects. Finally, momentum transfer distributions are compared in Fig. 4c with the prediction of the Primakoff formalism (experimental $p_T$ resolutions have been folded into the theoretical distribution). The good agreement indicates that the data are indeed dominated by Coulomb production.

The integrated cross-sections for reactions (2.13) are given in Table I, together with corresponding predictions of the one-photon-exchange model. As expected from our discussion of the differential cross-sections, the agreement is good for all targets and for both positive and negative beam pions. The presence of any measurable two-photon exchanges, neglected in the Primakoff formulae, could have spoiled this agreement. The size of the two-photon exchange contributions depends on the target nucleus and on the sign of the beam particle (in case of the interference term), and the absence of such dependencies, at the level of accuracy of the presented data, demonstrates that the one-photon exchange approximation is fully justified for the processes discussed in this paper. The weighted mean for the deviations of the measured from the expected values in Table I is $-(4\pm4)\%$. Consequently, the Primakoff formalism appears to be reliable to an accuracy of at least 8%, at an 84% confidence level.

The results of Refs [36, 37] are supported by a recent high-statistics study of reaction (2.13) at 43 GeV at Serpukhov [53]. Unfortunately, the normalization of that experiment was uncertain to $\approx15\%$ and, consequently, it could not be used to further improve the
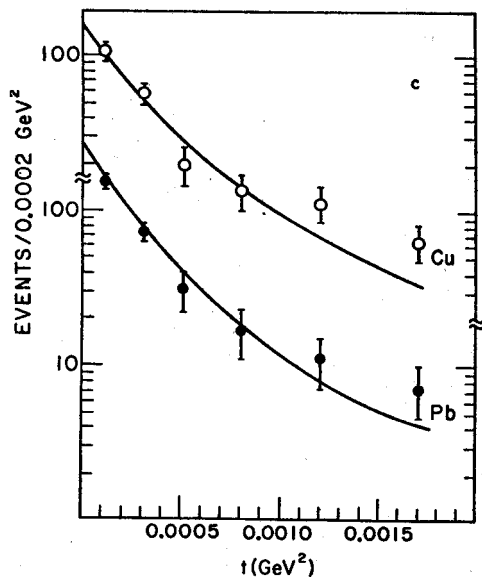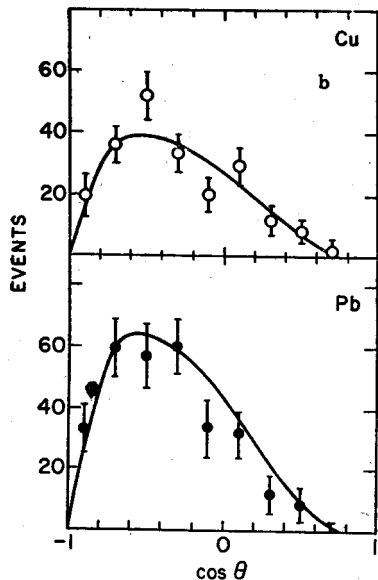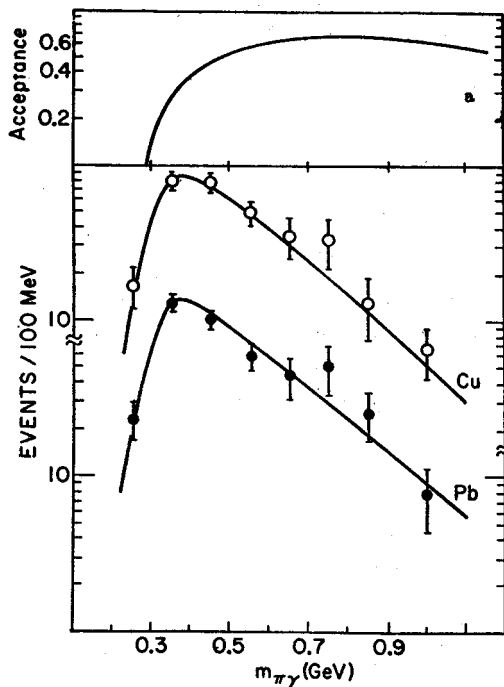
Fig. 4. (a) Mass spectrum of $\pi^+\gamma$ systems produced coherently on Cu and Pb at 200 GeV [37], for $t < 0.001$ GeV². (b) Angular distributions of $\pi^+$ in the $\pi^+\gamma$ rest frame. Data are for $t < 0.001$ GeV² and $0.3 < m_{\pi\gamma} < 0.6$ GeV. (c) $t$-distributions of $\pi^+\gamma$ systems, for $0.3 < m_{\pi\gamma} < 0.6$ GeV. Absolute predictions from the Primakoff formalism (assuming point pions) are given by the smooth curves

above estimate of the accuracy of the Primakoff method. Nonetheless, I quote the result of Ref. [53] for the ratio of the measured to the theoretical cross-sections of $0.96 \pm 0.15$, averaged over $\pi\gamma$ mass between 0.12 and 0.6 GeV. It seems worth mentioning that the precision measurement of the relative photon energy spectra in the 40 GeV data [53] was sensitive to pion-structure effects. These were observed as deviations in the shapes of the photon energy distributions from the predictions that assumed a point-like pion. Such deviations can be interpreted in terms of electric and magnetic pion polarizabilities, which define induced dipole moments of a particle in an electromagnetic field.

Additional checks on the Primakoff method are provided by measurements of radiative widths that use other techniques. The most accurate recent test of this kind was provided by a direct measurement of the $\pi^0$ lifetime [16], which gives $\Gamma(\pi^0 \to \gamma\gamma) = 7.25 \pm 0.18 \pm 0.11$ eV, compared to the average of two most recent Primakoff results [25, 26] of 7.7 $\pm 0.3$ eV. It should be noted, however, that the determinations of the $2\gamma$ width of the $\eta$ meson using two-photon $e^+e^-$ data [10] differ from the most accurate Primakoff measurement [27] by about three standard deviations. These results are presented in more detail in Section 3.

For completeness, I mention also results of tests of the Primakoff formalism based

TABLE I

Measured and predicted cross-sections for electromagnetic processes $\pi^\pm A \to \pi^\pm \gamma A$ [36, 37]. Errors on experimental values combine statistical and systematic uncertainties in quadrature. Errors on theoretical values are due to estimated uncertainties in parametrizations of nuclear form factors

| Interaction | Experiment (mb) | Theory (mb) | Integration range $t$ (GeV$^2$) $m$ (GeV) |
|---|---|---|---|
| $\pi^+$Cu | $0.0358 \pm 0.0030$ | $0.0345 \pm 0.0007$ | $t < 0.001,\ 0.3 < m < 1.2$ |
| $\pi^+$Pb | $0.252 \pm 0.021$ | $0.271 \pm 0.005$ | $t < 0.001,\ 0.3 < m < 1.2$ |
| $\pi^-$Cu | $0.029 \pm 0.006$ | $0.035 \pm 0.004$ | $t < 0.002,\ 0.3 < m < 2.0$ |
| $\pi^-$Pb | $0.249 \pm 0.027$ | $0.268 \pm 0.018$ | $t < 0.002,\ 0.3 < m < 2.0$ |

TABLE II

Comparison of recent measurements of the $\rho$ meson radiative width. Results of Ref. [32] that were obtained with the same target material and at the same beam energy were combined as weighted averages

| Interaction | Energy (GeV) | $\Gamma(\rho \to \pi\gamma)$ (keV) | Ref. |
|---|---|---|---|
| $\pi^+$C | 200 | $47.3 \pm 7 \pm 3$ | [39] |
| $\pi^+$Cu | 200 | $59.5 \pm 1.9 \pm 3.8$ | [39] |
| $\pi^+$Pb | 200 | $59.3 \pm 1.6 \pm 3.8$ | [39] |
| $\pi^-$Pb | 200 | $66.6 \pm 8.5$ | [55] |
| $\pi^-$C | 156 | $77.5 \pm 7.8 \pm 7.1$ | [32] |
| $\pi^-$Al | 156 | $88.2 \pm 10 \pm 8$ | [32] |
| $\pi^-$Cu | 156 | $68.5 \pm 3.8 \pm 6.2$ | [32] |
| $\pi^-$Pb | 156 | $76.7 \pm 3.6 \pm 7$ | [32] |
| $\pi^-$Cu | 260 | $74.5 \pm 8 \pm 6.8$ | [32] |
| $\pi^-$Pb | 260 | $60.5 \pm 4.1 \pm 5.5$ | [32] |

on the Coulomb production of the $\Delta^+$ resonances by incident protons [32, 54]. The sensitivity of these tests was limited by experimental acceptance, uncertainties in resolution, by the input cross-section for $\gamma p \rightarrow p\pi^0$, and by potential backgrounds from diffractive production (e.g., $N^*(1400)$). The examined data [32, 54] were found consistent with dominant Coulombic production of the $\Delta^+$, and agreement with absolute predictions of the Primakoff formalism was demonstrated at $\approx 10\%$ level.

Indirect support for the validity of the Primakoff technique is also provided through detailed comparisons of radiative widths of mesons and their consistency, as determined on different targets, at different energies, and for both charges of beam particles. I collect the most recent results for the best studied case of the $\varrho$ meson in Table II. Taking into account both the statistical and (more difficult to determine precisely) systematic errors a fairly good agreement between different measurements is observed.

I conclude that there is overwhelming proof that the Primakoff method can be used reliably for extracting radiative widths of mesons.

## 3. Radiative decays of vector and pseudoscalar mesons

Radiative decays involving vector (V) and pseudoscalar (P) mesons are presented separately from tensor (T) and axial (A) decays; this is done because the analysis of the P and V transitions is simpler in most models. Before discussing consequences of these decays for meson phenomenology, I will give a short account of recent measurements.

### 3.1. Recent experimental data

In the past few years, several precision measurements of vector and pseudoscalar radiative widths have been completed. Of special importance are results for widths of charged mesons. Decays of such mesons are not affected by mixing that is present for the isoscalar sector, and, consequently, charged-particle decays provide stronger constraints for models.

Until recently information on radiative decays of most charged mesons was either missing or inaccurate. New data include decays of $\varrho^+ \rightarrow \pi^+\gamma$, $\varrho^- \rightarrow \pi^-\gamma$, $K^{*+} \rightarrow K^+\gamma$; in all cases the radiative widths have been measured using the Primakoff method.

For the charged $\varrho$, the new values obtained by the Rochester–Minnesota–Fermilab collaboration are $\Gamma(\varrho^+ \rightarrow \pi^+\gamma) = 59.8 \pm 4$ keV [39] and $\Gamma(\varrho^- \rightarrow \pi^-\gamma) = 71 \pm 7$ keV [32], with the weighted average of $63 \pm 4$ keV. This result is in agreement with a recent measurement at CERN [55] $\Gamma(\varrho^- \rightarrow \pi^-\gamma) = 65 \pm 10$ keV, and it supersedes an older value of $35 \pm 10$ keV [54]. As it was pointed out in [34], the older value of the radiative width of the $\varrho^-$ could have been caused because possible $A_2$-exchange contributions to the production of the $\varrho$ were neglected in the analysis of Ref. [54]. The new value of $63 \pm 4$ keV removes a sharp contradiction between experiment and most model predictions, which typically place $\Gamma(\varrho^- \rightarrow \pi^-\gamma)$ in the range of 60–120 keV. At the same time, this result clearly demonstrates the existence of a mechanism that suppresses radiative decay rates compared to expectations from nonrelativistic quark models. This point is elaborated upon in the next subsection.

As an aside, the clean and unique Primakoff regime of production of exclusive $\varrho$-meson final states in the measurement [39] (cf. Fig. 5), also provided an accurate extraction of the values of the $\varrho$-meson mass and total width. The obtained parameters, $m_\varrho = 771 \pm 4$ MeV and $\Gamma(\varrho \to \pi\pi) = 150 \pm 5$ MeV agree well with corresponding world averages [56]. I note that the expected distortion of the resonance shape, due to mass dependent factors (other than just the Breit-Wigner term) in the Primakoff production formula (2.7) is clearly seen in the data, and this result again substantiates the validity of this technique.

The radiative width of the charged K*(890) was measured in the same experiment to be $\Gamma(K^{*+} \to K^+\gamma) = 51 \pm 5$ keV [47]. Recently, a remeasurement [57] of $\Gamma(K^{*0} \to K^0\gamma)$ provided the value of $116.5 \pm 9.9$ keV, much improved relative to the previously accepted value of $75 \pm 35$ keV [58]. Because of the presence of strange quarks, the radiative widths of the K* mesons are sensitive to details of SU(3) breaking pattern. With radiative widths of both charged and neutral K* accurately measured, one can compare the ratio of the two widths to various predictions. In such ratios, uncertainties from overall theoretical normalization factors tend to cancel (see below).

A significant reduction of errors on the radiative decay widths of the $\phi$ meson has
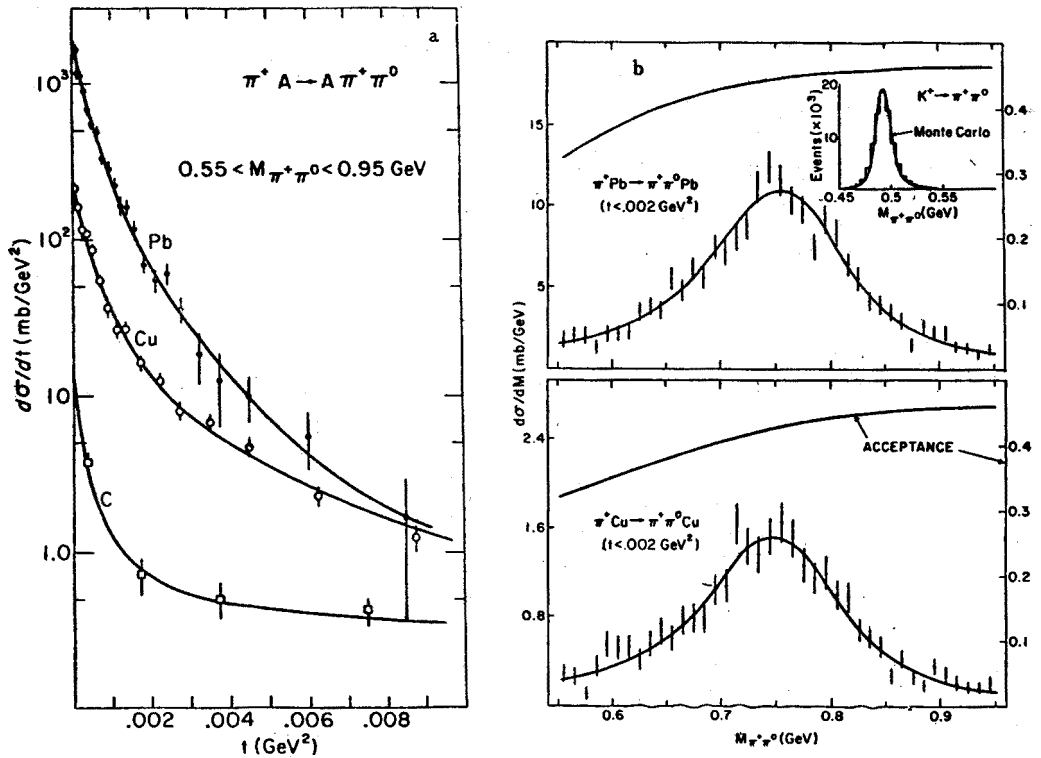


Fig. 5. (a) $t$-distributions for $\pi^+\pi^0$ systems produced coherently on Cu and Pb targets at 200 GeV, and fits of Eq. (2.12) to the data [39]. (b) Mass distributions for $\pi^+\pi^0$ systems and fits used to establish the $\rho^+$ mass and full width [39]. The insert displays the mass distribution observed for tagged $K^+ \to \pi^+\pi^0$ decays in the beam, and a Monte Carlo of the expected distribution

TABLE III

Comparison of experimental data on radiative widths of pseudoscalar and vector mesons with several theoretical calculations. All values of the radiative widths are given in keV. Experimental values were taken from [56], unless specified otherwise

| Decay | Experiment | Ono [65] | Godfrey [68] | Ishida [73] | Ohshima [79] | Filippov [13] | Gomm [89] |
|---|---|---|---|---|---|---|---|
| $\rho^\pm \to \pi^\pm\gamma$ | $63\pm4$ [39] | 78 | 68 | 68 | $67\pm7$ | 58 | 80 |
| $\rho^0 \to \eta\gamma$ | $52\pm13$ | 50 | 44 | 40 | $45.6\pm21.7$ | 54 | 38 |
| $K^{*\pm} \to K^\pm\gamma$ | $50.5\pm4.6$ | 109 | 67 | 78 | $37.5\pm4$ | 33 | 29 |
| $K^{*0} \to K^0\gamma$ | $116.5\pm9.9$ | 140 | 117 | 122 | $147\pm16$ | 130 | 117 |
| $\omega \to \pi^0\gamma$ | $853\pm49$ / $789\pm92$ [79] | 739 | 650 | 649 | $789\pm120$ | 825 | 800 |
| $\omega \to \eta\gamma$ | $2.9^{+2.5}_{-1.8}$ | 6.5 | 5.4 | 5.2 | $9.0\pm2.5$ | 8.3 | 5 |
| $\eta' \to \rho^0\gamma$ | $72\pm12$ | 111 | 139 | 87 | $93.1\pm24.1$ | 78 | 77 |
| $\eta' \to \omega\gamma$ | $6.5\pm1.5$ | 10 | 13.2 | 8 | $8.4\pm2.4$ | 7.2 | 7 |
| $\phi \to \eta\gamma$ | $54\pm4.5$ | 62 | 66 | 72 | $137\pm18$ | 71 | 68 |
| $\phi \to \pi^0\gamma$ | $5.5\pm0.6$ | 0 | 1.2 | 0 | $11.1\pm14.5$ | 6 | 5 |
| $\pi^0 \to \gamma\gamma$ | $(7.34\pm0.33)\cdot10^{-3}$ | | $6.8\cdot10^{-3}$ | | | $7,3\cdot10^{-3}$ | |
| $\eta \to \gamma\gamma$ | $0.55\pm0.053$ [10] / $0.32\pm0.046$ [27] | | 0.25 | | | 0.72 | |
| $\eta' \to \gamma\gamma$ | $4.5\pm0.37$ | | 1.7 | | | 7.5 | |
| $\iota \to \gamma\gamma$ | see text | | | | | | |
| $\iota \to \rho\gamma$ | see text | | | | | | |

been achieved in the most recent measurement of Ref. [22]; the values $\Gamma(\phi \to \gamma\gamma)$ = 55±3 keV and $\Gamma(\phi \to \pi^0\gamma)$ = 5.5±0.6 keV were obtained.

In the isoscalar sector, new results for $\Gamma(\eta \to \gamma\gamma)$ and $\Gamma(\eta' \to \gamma\gamma)$ have been obtained from $\gamma\gamma$ data in $e^+e^-$ collision experiments. The weighted averages for the $\gamma\gamma$ results are $\Gamma(\eta' \to \gamma\gamma)$ = 4.17±0.33 keV and $\Gamma(\eta \to \gamma\gamma)$ = 0.55±0.053 keV [10]. The latter value disagrees with an earlier Primakoff measurement of $\Gamma(\eta \to \gamma\gamma)$ = 0.324±0.046 keV [27]. This discrepancy must be resolved to obtain reliable determinations of pseudoscalar mixing angles from two photon widths of the $\eta$ and $\eta'$, and for evaluating possible glueball (or other "inert") admixtures to the wave functions of these states [15]. A recent measurement of $\Gamma(\pi^0 \to \gamma\gamma)$ width has been presented in Section 2.1.

The experimental values quoted in this Section are taken into account in Table III, together with the older values of other vector and pseudoscalar radiative widths. Selected results from several representative theoretical models are also presented in Table III.

## 3.2. Theoretical models

Radiative decays of mesons have been discussed for over two decades, using many diverse approaches. The main framework of this effort has been based on ideas from quark models, unitary symmetry schemes, current algebra and effective low-energy Lagrangians. Often, Vector Dominance Models (VDM) have been used to relate photon and hadronic couplings. Rather than attempting an exhaustive presentation of this vast field of research I will concentrate only on recent developments. References to earlier work can be found in the quoted literature, especially in the review papers [11, 12, 13].

### QUARK MODELS

Most of the recent calculations of vector and pseudoscalar radiative decays were performed within different versions of the quark model. I begin with a discussion of a basic scheme for V → Pγ transitions [59, 60], in which these decays are described as magnetic dipole transitions in the q$\bar{\text{q}}$ system (in analogy with M1 transitions in hydrogen-like atoms). In a nonrelativistic, long-wavelength approximation the result for the radiative widths is

$$\Gamma(\text{V} \to \text{P}\gamma) = \tfrac{4}{3} \alpha k^3 \mu_{\text{PV}}^2 f, \tag{3.1}$$

where $k$ is the decay momentum in the rest frame of V and $\mu_{\text{PV}}$ represents matrix element of the magnetic moment transition operator between the vector and pseudoscalar states. In terms of quark magnetic moments $\mu_q$, it can be expressed as:

$$\mu_{\text{PV}} = \langle \text{P}|\hat{\mu}|\text{V}\rangle = \langle \text{P}|\sum_q \mu_q e_q \hat{\sigma}_{qz}|\text{V}\rangle, \tag{3.2}$$

where $\hat{\sigma}_q$ are Pauli matrices and $e_q$ are charges of the quarks in units of the elementary charge. In this notation $\mu_q = g_q/2m_q$, $g_q$ being the quark gyromagnetic factor, and the proton magnetic moment is $\mu_p = 2.79/2m_p$. If unbroken SU(3) is assumed, one obtains $\mu_q = \mu_p$ for q = u, d, s. Alternatively, $\mu_u$, $\mu_d$, $\mu_s$ can be determined from the magnetic moments of p, n and $\Lambda$. The latter procedure takes into account symmetry breaking in the values of baryon magnetic moments, and relates radiative widths of mesons to properties

of baryons. It should be recognized, however, that no fully satisfactory (i.e. better than to 10–20%) description of baryon magnetic moments has been achieved to date [61]. Any calculation of meson widths, using input from baryon magnetic moments, bears corresponding uncertainties. Below, I will also discuss other problems of this approach.

There is a still unresolved controversy concerning the factor $f$ in Eq. (3.1). The original calculation [59] obtained formula (3.1) using both relativistic phase-space and a relativistic $P \to V\gamma$ vertex, which can be written in the form [62]:

$$2\mu_{PV}\partial_\alpha A_\beta \partial_\mu V_\nu P\varepsilon^{\alpha\beta\mu\nu} f^{1/2}, \tag{3.3}$$

where $f$ is a Lorentz-scalar function $f = f(m_V, m_P)$, and $A_\mu$, $V_\mu$, $P$ are electromagnetic, vector-meson, and pseudoscalar-meson fields, respectively. The factor $f$ was originally determined in the limiting case $m_V = m_P = m$, by requesting that the relativistic amplitude reduce to the well-known expression for the nonrelativistic M1-transition in the long-wavelength approximation:

$$T^{(LW)} = \frac{1}{\sqrt{2k}} \vec{\mu} \cdot (\vec{k} \times \vec{\varepsilon}). \tag{3.4}$$

In this limit, one obtains $f(m, m) = 1$. If a weak dependence is assumed for $f$ on its arguments, such that $f \approx 1$ even for physical values of vector and pseudoscalar masses, then one obtains $\Gamma(\varrho^+ \to \pi^+\gamma) \approx 123$ keV (or $\approx 111$ keV if SU(3) breaking of baryon magnetic moments is taken into account). These values constitute original predictions of the quark model [59, 60]. The experimental value of $63\pm4$ keV is significantly lower.

A different attitude has been proposed in Ref. [12]. There, it was assumed that the relativistic matrix element can be approximated by the nonrelativistic M1-transition amplitude at the physical value of the masses. Since, in the rest frame of a V that is polarized along the $+z$ axis, the amplitudes are related by [62]:

$$T^{(REL)}(V \to P\gamma) \approx T^{(LW)}(V \to P\gamma)f^{1/2}\sqrt{\frac{m_V}{E_P}}; \tag{3.5}$$

for this relationship to hold, the factor $f$ must equal $E_P/m_V$. In the case of $\varrho \to \pi\gamma$ decay, this factor is $E_\pi/m_\varrho \approx 0.52$, and, consequently, $\Gamma(\varrho^+ \to \pi^+\gamma)$ is predicted to be $\approx 64$ keV ($\approx 58$ keV in case of broken SU(3)). These $f$-factors have similar magnitude for the other radiative transitions, and, in general, improve the agreement of Eq. (3.1) with experiment. Nevertheless, although the factor $f(m_V, m_P)$ may, in fact, differ from unity for physical masses of particles, the specific prescription $f = E_P/m_V$ cannot be fully justified [62]. One may conclude therefore that, with no satisfactory relativistic treatment of the quark model, the above calculations of meson radiative widths are subject to uncertainty by about factors of two.

A phenomenological way to skirt this problem is to use Eq. (3.1) for testing ratios of radiative widths of particles with similar decay kinematics and same quark content, e.g. $\Gamma(\omega \to \pi\gamma)/\Gamma(\varrho \to \pi\gamma)$ or $\Gamma(K^{*+} \to K^+\gamma)/\Gamma(K^{*0} \to K^0\gamma)$. In such ratios, the above ambiguity tends to cancel out. I present the result of such a comparison in Table IV. For the ratios, the agreement between Eq. (3.1) and experiment is clearly very reasonable. The

TABLE IV

Comparison of data with predictions from SU(3) for ratios of radiative widths of vector mesons. Experimental values were taken from Refs [39, 57]

| Ratio | Experiment | Unbroken SU(3) | Broken SU(3) |
|---|---|---|---|
| $\dfrac{\Gamma(\omega \to \pi^0\gamma)}{\Gamma(\varrho^+ \to \pi^+\gamma)}$ | $12.5 \pm 1.7$ | 9.6 | 10.9 |
| $\dfrac{\Gamma(K^{*0} \to K^0\gamma)}{\Gamma(K^{*+} \to K^+\gamma)}$ | $2.28 \pm 0.29$ | 4.0 | 1.64 |

error on the ratio of $\Gamma(\omega \to \pi\gamma)/\Gamma(\varrho \to \pi\gamma)$ is too large to distinguish between the predictions of broken and unbroken SU(3), but the recent measurements of the radiative widths of the $K^{*+}(890)$ and $K^{*0}(890)$ appear to be in better agreement with the prediction of broken symmetry.

The data on absolute values of vector and pseudoscalar radiative widths clearly require a suppression, that is $f < 1$ in Eq. (3.1). It makes it interesting to explore different possible mechanisms for such suppression, especially because its explanation through the phase-space factor $E/m$ is not well motivated.

One line of argument relates the needed suppression to the presence of spin-dependent quark-quark forces; this arises naturally in QCD-based models of hadrons in which quark interactions are mediated by gluon exchanges [8, 9, 63]. A lesson learned from heavy-quark mesons, where $(v/c)^2$ relativistic corrections to the interaction Hamiltonian can be reliably introduced in a perturbative way, has been that relativistic modifications of meson wave-functions can result in a significant suppression of certain radiative decay widths [64]. A similar approach has been taken for the radiative decays of light mesons [65, 66, 67]. The major calculated effect was found to be caused by spin-spin interactions affecting the scale of the spatial extent of meson wave functions. Such interactions are repulsive for spin-triplet states and attractive for singlet states, so, consequently, $\langle r \rangle_V > \langle r \rangle_P$ and overlaps of spatial wave functions decrease:

$$f = \int d^3 r \psi_V^*(\vec{r}) \psi_P(\vec{r}) < 1. \qquad (3.6)$$

The overlap factors $f$ were calculated numerically and, incorporating them into Eq. (3.1), provides a reasonable description of radiative transitions for $V \to P\gamma$ and $P \to V\gamma$. As an example, I present the results of Ref. [65] in Table III.

A generalization of this approach led to a common, QCD-based, description of radiative decays, as well as other meson systematics. A detailed study of meson properties (mass spectra, strong, electromagnetic and weak couplings) in such a model [68] demonstrated that all mesons (light and heavy) can be successfully described within a single scheme. In Ref. [68] mesons are represented in terms of rest-frame valence quark configurations, with dynamics governed by a relativistic Hamiltonian. The Hamiltonian of the model reproduces, in the nonrelativistic limit, a one-gluon exchange potential at short distances, a Lorentz-scalar confinement term, and spin-dependent interactions of the expected form.

The main relativistic effects have been parametrized by introducing a dependence of the interaction strength on the energy of the interacting quarks, and by modifying the spatial shape of the potentials through appropriate smearing of the interquark coordinates. Although only approximate, these relativization procedures have been argued to capture most of the essential features of relativistic effects for systems with momentum-to-mass ratio $p/m \approx 1$, which are not too far from the nonrelativistic regime. A possibility for mixing of quark configurations was also introduced through the annihilation interaction $q\bar{q} \leftrightarrow$ gluons. The same model provides a good description of the known baryons, with parameters very similar to those determined in the meson sector [69]. Similar approaches have been used widely for describing less relativistic $c\bar{c}$ and $b\bar{b}$ systems.

In Table III, I include the results of Ref. [68] for meson radiative widths. Correct description of this sector was found sensitive to relativistic features of the model. Besides imposing the above relativization procedure, the Hamiltonian of electromagnetic interactions was also modified in accord with the general philosophy of this approach. The major modification can be represented by replacement of (static) $1/m$ factors in the definition of quark magnetic moments by (effective) $1/E$ denominators.

As can be seen from Tables III and V, other, much simpler, models focused solely on describing radiative decays of mesons, can achieve comparable (or better) overall quantitative agreement with the data. The major advantage of the model of Ref. [68] is, of course, its wide scope of applications and its close relation to basic theory of strong interactions, QCD. For radiative transitions, discrepancies with experiment occur, in particular, for decays sensitive to mixing of quark configurations, i.e. those involving $\eta$, $\eta'$ and OZI-suppressed $\phi$ decays. This indicates that the annihilation mixing mechanism of Ref. [68] needs to be refined.

Since the photon emission by mesons is theoretically more straightforward than their hadronic decays, I believe that further developments of QCD-based models should benefit from detailed analysis of radiative decay channels. In particular, one may hope for a better formulation of relativistic modifications to the quark model, attempted, but not fully achieved, within the approach of Refs. [68, 70] (see also references quoted therein).

Several relativistic calculations of meson radiative widths have been based on the relativistic harmonic oscillator quark model, in the spirit of work by Feynman, Kislinger and Ravndall [71]. It has been pointed out [72] that in such an approach one can expect significant recoil corrections to radiative decay rates, due to relativistic velocities of the final state mesons in most $V \to P\gamma$ and $P \to V\gamma$ transitions. However, the agreement between the results of Ref. [72] and more recent data is not very good. It is not known if this calculation could be adjusted to fit the data a-posteriori.

A related approach has been developed in a covariant oscillator quark model [73] that provides a direct relation between radiative decay amplitudes and hadronic currents involved in the decay process. The results (see Table III) are generally in fair agreement with data, without introducing ad hoc suppression factors needed in nonrelativistic quark model calculations [12, 74].

One may conclude that radiative decays of mesons provide a sensitive testing ground for attempts to formulate relativistic quark models of hadrons.

Without going into details of the meson quark structure, radiative decays of light mesons can be interrelated through unitary symmetry schemes. In this approach, radiative decays provide tests of various symmetry breaking mechanisms that have been proposed in the literature.

The starting point for discussing symmetry breaking is, of course, the unbroken case. SU(3) symmetry has been widely used to relate hadronic couplings between vector and pseudoscalar states. This can be extended to incorporate photon couplings, with the usual assumption that the photon is a pure $U = 0$ member of an SU(3) octet [75, 76, 77]. The $g_{PV\gamma}$ couplings are then related as follows:

$$g_{ijk} \propto \langle V_i | j_j(0) | P_k \rangle \propto \frac{2eg}{m_\pi} d_{ijk}, \tag{3.7}$$

where $j(x)$ represents the electromagnetic current and $d_{ijk}$ are the usual SU(3) coefficients (for sake of simplicity, Lorentz structure of Eq. (3.7) has been suppressed). Consequently, one obtains

$$\frac{g}{3} = g_{\varrho^0\pi^0\gamma} = g_{\varrho^\pm\pi^\pm\gamma} = g_{K^{*\pm}K^\pm\gamma} = -\tfrac{1}{2} g_{K^{*0}K^0\gamma} = \frac{1}{\sqrt{3}} g_{\omega_8\pi^0\gamma} = \frac{1}{\sqrt{3}} g_{\varrho^0\eta_8\gamma} = -g_{\omega_8\eta_8\gamma}. \tag{3.8}$$

Taking into account that the photon is a $U$-spin singlet, one obtains for $V_8P_1\gamma$ couplings [3, 78]

$$g_{\varrho\eta_1\gamma} = \sqrt{3} g_{\omega_8\eta_1\gamma} \equiv \sqrt{\tfrac{2}{3}} g'_1, \tag{3.9}$$

and a similar relation for $V_1P_8\gamma$ couplings

$$g_{\omega_1\pi^0\gamma} = \sqrt{3} g_{\omega_1\eta_8\gamma} \equiv \sqrt{\tfrac{2}{3}} g_1 \tag{3.10}$$

(subscripts 1 and 8 denote singlet and octet states, respectively). Taking into account mixing of singlet and octet components, both in pseudoscalar and vector sectors, for the physical states we write:

$$\eta = \eta_8 \cos \theta_P - \eta_1 \sin \theta_P, \qquad \eta' = \eta_8 \sin \theta_P + \eta_1 \cos \theta_P, \tag{3.11}$$

$$\phi = \omega_8 \cos \theta_V - \omega_1 \sin \theta_V, \qquad \omega = \omega_8 \sin \theta_V + \omega_1 \cos \theta_V. \tag{3.12}$$

Substituting these relations into (3.8)–(3.10) it is straightforward to derive relations between the couplings of physical particles (see e.g. [12] for rather lengthy formulae). The radiative widths of mesons are then expressed through these couplings as follows

$$\Gamma(V \to P\gamma) = \tfrac{4}{3} \alpha \frac{k^3}{m_\pi^2} |g_{VP\gamma}|^2, \tag{3.13}$$

$$\Gamma(P \to V\gamma) = 4\alpha \frac{k^3}{m_\pi^2} |g_{PV\gamma}|^2, \tag{3.14}$$

where $k$, as before, is the decay momentum in the rest frame of the initial state particle. A "minimal" prescription for symmetry breaking consists of using physical masses in the calculation of $k$. Additional breaking can be easily introduced by foresaking nonet symmetry and allowing the couplings $g$, $g_1$ and $g_1'$ to differ. Even this simple scheme provides a reasonable description of the radiative widths; in Table III, I show results of such a calculation [79], with broken nonet symmetry and mixing angles taken to correspond to ideal vector mixing $\theta_V = 35.3°$, and pseudoscalar mixing consistent with a quadratic mass formula, namely $\theta_P \approx -11°$. Major disagreement with data occurs for $\phi \to \eta\gamma$ and $K^{*0} \to K^0\gamma$ decays; in both cases the calculated decay widths are too large. The $K^*$ radiative decay widths can be reduced by breaking SU(3) and isospin symmetries through the quark masses [80].

To improve the agreement with data, various other prescriptions for symmetry breaking have been proposed. In Ref. [81] a symmetry breaking spurion interaction has been considered. In the model of Ref. [13], OZI-rule breaking transitions and SU(3) breaking by intermediate virtual-meson state are introduced. Although such prescriptions can achieve somewhat better agreement with data, such schemes do not provide any clear advantage, and the price of introducing additional free parameters is probably not justified by the obtained improvements. Moreover, a realistic description of meson wave functions is very likely to involve other ingredients than just the standard SU(3) states; for example, various schemes, that mix ground states of basic multiplets with their radial excitations and/or glueball states, are currently in active consideration (see below for additional details).

Interesting extensions of symmetry relationships can be achieved with the help of Vector Dominance Models (VDM). Relevant ideas are reviewed in detail, e.g., in [5, 12]. This approach assumes that any soft interaction of photons with hadrons proceeds via an intermediate virtual vector meson state; dominant contributions are expected to come from the lightest mesons, such as $\varrho^0$, $\omega$, and $\phi$. The transition couplings between the photon and the vector mesons are conventionally defined by a relation between corresponding currents ($j^\mu$, again, being the electromagnetic current):

$$j^\mu(x) = \frac{em_\varrho^2}{2\gamma_\varrho}\,\varrho^\mu(x) + \frac{em_\omega^2}{2\sqrt{3}\,\gamma_Y}\,\omega^\mu(x)\sin\theta_V + \frac{em_\phi^2}{2\sqrt{3}\,\gamma_Y}\,\phi^\mu(x)\cos\theta_V. \tag{3.15}$$

For exact SU(3), $\gamma_\varrho = \gamma_Y$ and, in case of ideal vector mixing, $\theta_V = \arctan\left(\frac{1}{\sqrt{2}}\right)$. One way of determining the $V-\gamma$ couplings is from the measured width of the $\varrho^0 \to e^+e^-$ decay. Using the above conventions, we can write:

$$\Gamma(\varrho^0 \to e^+e^-) \approx \frac{\pi\alpha^2}{3}\,\frac{m_\varrho}{\gamma_\varrho^2}, \tag{3.16}$$

which yields $\gamma_\varrho^2/\pi = 1.98 \pm 0.09$. Another estimate follows from the equality $\gamma_\varrho = \gamma_{\varrho\pi\pi}$, which is required within the VDM approach by the $F_\pi(0) = 1$ constraint on the pion form

factor. Here, $\gamma_{\varrho\pi\pi}$ is the $\varrho\pi\pi$ hadronic coupling, related to the $\Gamma(\varrho \to \pi\pi)$ width by:

$$\Gamma(\varrho^0 \to \pi^+\pi^-) = \tfrac{2}{3} \frac{\gamma_{\varrho\pi\pi}^2}{\pi} \frac{k^3}{m_\varrho^2}. \tag{3.17}$$

This yields $\gamma_\varrho^2/\pi \approx 3.0$ (see also [82] for similar estimates). Several other determinations, e.g. involving comparisons of ($\omega \to \pi^0\gamma$ and $\pi^0 \to \gamma\gamma$) or ($\omega \to 3\pi$ and $\omega \to \pi^0\gamma$) provide intermediate values of $\gamma_\varrho^2/\pi$. Consequently, I use below $\gamma_\varrho^2/\pi = 2.5 \pm 0.5$ as a conservative estimate.

As an example of the application of VDM, let us consider the relation between $\varrho^+ \to \pi^+\gamma$ and $\pi^0 \to \gamma\gamma$ decays. The constant $g_{\pi\gamma\gamma}$ can be easily calculated from $g_{\pi\varrho\gamma}$ and $g_{\pi\omega\gamma}$ by considering the couplings of the vector particles to the photon, according to the VDM prescription

$$g_{\pi\gamma\gamma} = \frac{e}{2\gamma_\varrho} g_{\pi\varrho\gamma} + \frac{e}{2\sqrt{3}\,\gamma_Y} g_{\pi\omega\gamma} \simeq \frac{e}{\gamma_\varrho} g_{\pi\varrho\gamma}, \tag{3.18}$$

where in the last step an unbroken nonet relation has been used. Consequently, one obtains the ratio of the widths

$$\frac{\Gamma(\varrho^+ \to \pi^+\gamma)}{\Gamma(\pi^0 \to \gamma\gamma)} = \frac{4}{3\alpha} \frac{\gamma_\varrho^2}{\pi} \left(\frac{k}{m_\pi}\right)^3. \tag{3.19}$$

Using $\Gamma(\pi^0 \to \gamma\gamma) = 7.34 \pm 0.33$ eV [56], and $\gamma_\varrho^2/\pi$ as specified above, the expected value of $\Gamma(\varrho^+ \to \pi^+\gamma)$ becomes $63 \pm 12$ keV. The agreement with the experimental value of $63 \pm 4$ keV is very reasonable, and far better than that of the naive ($f = 1$) nonrelativistic quark model (i.e. 120 keV), although the uncertainty introduced because of different evaluations of $\gamma_\varrho^2/\pi$ is uncomfortably large. As seen from Table III, SU(3) extensions of this result to other radiative decays, with [13] or without [79] symmetry breaking, account for the major patterns of the data. In Ref. [83], a VDM analysis was performed with the values of $\gamma_\varrho$ and $\gamma_{\varrho\pi\pi}$ left unrelated. It should be pointed out that this and other generalized versions of VDM were developed, typically, before new data on radiative meson decays became available (see, e.g., [84, 85]). Because data have now attained a high level of accuracy, they can provide an excellent laboratory for testing of models of SU(3)-breaking and/or VDM extensions, and the old fits should therefore be reexamined.

CHIRAL ANOMALIES AND LOW-ENERGY EFFECTIVE LAGRANGIANS

The above VDM relation of $\pi^0 \to \gamma\gamma$ to other electromagnetic decays of mesons is of particular interest since the absolute value of the two-photon width of the $\pi^0$ is calculable from the theory of chiral anomalies [86, 87]. The result of the calculation is in good agreement with experiment:

$$\Gamma(\pi^0 \to \gamma\gamma) = \frac{\alpha^2}{64\pi^3} \left(\frac{m_\pi}{f_\pi}\right)^2 m_\pi \approx 7.6 \, \text{eV}, \tag{3.20}$$

where $f_\pi = 93$ MeV has been used. Using VDM and SU(3) symmetry relations, one can also obtain absolute predictions for other radiative widths.

Vector and axial mesons can be incorporated directly into a chiral Lagrangian as phenomenological gauge fields of flavor $SU(3)_L \otimes SU(3)_R$ symmetry [88]. This approach has been recently modified [89, 90] to include vector and axial gauge fields in the presence of the anomalous Wess-Zumino term. This extension is purported to increase the range of validity of the chiral-Lagrangian method up to masses of about 1 GeV. In the extended scheme, the gauged Wess-Zumino term describes the "anomalous" decays, for which the product of parities of particles taking part in the process is negative. Such processes include all VVP couplings, and, in particular, a large number of $V \to P\gamma$ decays. The interactions of photons were incorporated in the calculations using a VDM prescription, without the introduction of new coupling constants [89]. With symmetry breaking corrections, introduced by allowing somewhat different hadronic decay constants $F_K/F_\pi \approx F_\eta/F_\pi \approx 1.28$, the model [89] claims substantial phenomenological success. The results for $V \to P\gamma$ and $P \to V\gamma$ decays are included in Table III. The model also obtains some interesting results concerning the $A_1$ meson, that are deferred to the following Section.

The $P \to VV$, $V \to PV$ transitions have also been calculated [91] from quark triangle diagrams, assuming that the amplitude is dominated by anomalies, similar to those that determine the $\pi^0 \to \gamma\gamma$ decay probability in the current algebra framework. With no free parameters, except for a phenomenological suppression parameter $\lambda \approx 1.5$ for decays of particles involving strange quarks (using standard mixing angles), numerical results were obtained similar in quality to the ones discussed above. It is interesting that formulae obtained in this approach are identical to those of the nonrelativistic quark model, with effective u and d quark masses replaced by $4\pi^2 f_\pi/3\gamma_{\rho\pi\pi} \approx 410$ MeV and $m_s = \lambda m_u \approx 615$ MeV; these large mass values provide automatically the desired suppressions needed in the nonrelativistic quark model.

Recent experiments have tested yet another absolute prediction of the theory of chiral anomalies. This test concerns the coupling of the photon to 3 pions ($F_{3\pi}$) that, within the PCAC [92, 93] or the Wess-Zumino effective Lagrangian [94, 95, 96] frameworks, can be calculated to be:

$$F^{3\pi}(0) = \frac{eN_c}{12\pi^2 f_\pi^3} \approx 9.5 \text{ GeV}^{-3} \tag{3.21}$$

in the limit of zero pion-momenta ($N_c = 3$ is the number of colors).

Experimentally, the $F_{3\pi}$ coupling can be determined by the strength of the $\gamma\pi \to \pi\pi$ process, similar to the one employed to measure the $\varrho \to \pi\gamma$ decay via the Primakoff formalism. The major difference concerns the kinematics of the two measurements: $F_{3\pi}$ is determined at the two-pion production threshold, rather than at the mass of the $\varrho$. The measurement [97], based on the Primakoff method, reported $F_{3\pi}(0) = 13 \pm 0.9 \pm 1.3$ GeV$^{-3}$, in agreement with theoretical prediction for $N_c = 3$. This result is consistent with the one of Ref. [98], obtained from a similar measurement of $\pi e \to \pi\pi^0 e$ inelastic pion-electron scattering. The agreement between the two reactions can also be regarded as an additional check on the veracity of the Primakoff technique.

The overall picture that emerges, is that the theoretical methods that successfully predict the $\pi^0 \to \gamma\gamma$ width, when supplemented with VDM relations and approximate

SU(3) symmetry of couplings, also provide a description of most vector and pseudoscalar radiative widths accurate to about 20%. This agreement strengthens the argument that the factor-of-two discrepancies between data and the nonrelativistic quark model do not indicate any fundamental shortcomings of the theory. The values of $\Gamma(\pi^0 \to \gamma\gamma)$ and $F_{3\pi}$, discussed above, provide tests of implementations of the Wess-Zumino term in the effective chiral Lagrangians and help constrain various extensions of this scheme. This is particularly interesting in the context of the intensive development of this approach in studies of the low-energy limit of QCD and of soliton models of baryons [99].

### MIXING

I conclude the discussion of radiative decays of vector and pseudoscalar mesons with a few remarks on mixing of the neutral states. Such mixing has obvious impact on radiative widths and it can consequently be determined from such data. Since the radiative decay rates are sensitive to quark charges, they must, for example, reflect the quark composition of mesons.

While $\omega$–$\phi$ mixing in the vector sector is known to be almost ideal, the situation for the pseudoscalar nonet is much more ambiguous. Assuming simple orthogonal mixing (3.11), the two-photon widths of the $\eta$ and $\eta'$ mesons can be related to that of the $\pi^0$ as follows:

$$\Gamma(\eta \to \gamma\gamma) = \tfrac{1}{3} \Gamma(\pi^0 \to \gamma\gamma) \left(\frac{m_\eta}{m_{\pi^0}}\right)^3 (\cos\theta_P - \sqrt{8}\, R \sin\theta_P)^2, \qquad (3.22)$$

$$\Gamma(\eta' \to \gamma\gamma) = \tfrac{1}{3} \Gamma(\pi^0 \to \gamma\gamma) \left(\frac{m_{\eta'}}{m_{\pi^0}}\right)^3 (\sin\theta_P + \sqrt{8}\, R \cos\theta_P)^2. \qquad (3.23)$$

The parameter $R$ is given by the ratio of octet to singlet decay constants, and is indicative of nonet symmetry breaking if it differs from unity. Using the average $e^+e^-$ storage ring value of $\Gamma(\eta \to \gamma\gamma) = 0.55 \pm 0.053$ keV, and weighted averages for the other widths, one obtains [10]

$$R = 0.94 \pm 0.04 \quad \text{and} \quad \theta_P = -19.0 \pm 2.2°.$$

The above value of the pseudoscalar mixing angle $\theta_P$ is much larger than the usual one obtained from the Gell-Mann-Okubo quadratic mass formula ($\theta_P \approx -11°$).

Similarly large values of pseudoscalar mixing angles were obtained previously from analyses of hadronic processes involving the $\eta$ and $\eta'$ [100, 101, 102]. It was also realized before that non-orthogonal mixing schemes may be more appropriate for the $\eta - \eta'$ system [9, 103, 104], and that some additional "inert" component may mix with the basic configurations of the quark model. Either glueballs [103, 105, 106] or radial excitations [107, 108] (or both [109]) have been considered as sources for this component. (The related problem of $\iota(1460)$ mixing is discussed in Section 5.1.) In most of such schemes the $\eta$ appears as an almost pure quark state of usual composition, while the $\eta'$ requires a larger admixture of ground state $s\bar{s}$ quark configurations ($\theta_{\eta'} \approx -20°$) than is afforded by the GMO formula, and, in addition, a significant admixture of inert structure. These results emerge quite naturally from the point of view of the "nearest neighbor mixing" principle [107].

An updated analysis of new data on vector and pseudoscalar radiative decays and hadronic decays of J/$\psi$ within a three-component mixing scheme [106], has been presented by Roşner [15]. He writes

$$|\eta\rangle = X_\eta \left|\frac{u\bar{u}+d\bar{d}}{\sqrt{2}}\right\rangle + Y_\eta|s\bar{s}\rangle + Z_\eta|G\rangle \qquad (3.24)$$

and a similar expression for the $\eta'$. Various linear combinations of $X$'s and $Y$'s can be determined from the measured radiative widths. These constraints yield a solution such that $X_\eta^2 + Y_\eta^2$ is consistent with 1.0, and a pseudoscalar mixing angle $\theta_P$ of $\approx -20°$. The $\eta'$ data agree with such a large value of the mixing angle, but allow a significant ($\approx 65\%$) glue component in its composition.

The conclusion concerning the glue content of the $\eta$ and $\eta'$ mesons is supported independently by data on J/$\psi \to$ VP decays [110], where P and V stand for light (non--charmed) pseudoscalar and vector mesons. The J/$\psi$ decays are expected to proceed via a three-gluon intermediate state that couples to the quark lines of the final state mesons, V and P. Because of the OZI rule, in the dominant process, the quark lines are common to both final mesons, so that their quark content should be identical. Consequently, the process J/$\psi \to \eta\omega$ determines the nonstrange component of the $\eta$ while J/$\psi \to \eta\phi$ gives its strange component, etc. (here, one takes advantage of practically ideal mixing of the vector mesons). The analysis of Ref. [110] implies $X_\eta^2 + Y_\eta^2 = 1.1 \pm 0.2$, $X_{\eta'}^2 + Y_{\eta'}^2 = 0.65 \pm 0.18$ (cf. Fig. 6).
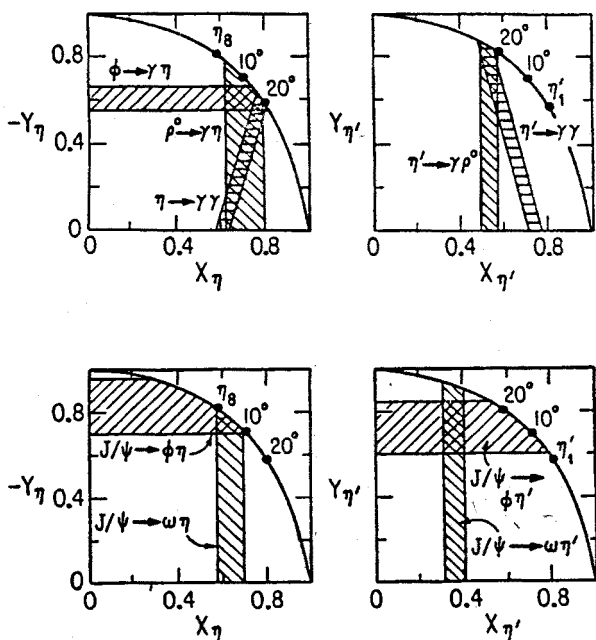


Fig. 6. Quark content of the $\eta$ and $\eta'$ from radiative processes involving only light quarks [15] and from hadronic decays of the J/$\psi$ [110]. The black dots indicate pure octet, pure singlet, or mixed states (labelled by mixing angle)

The discussion of pseudoscalar mixing is also affected by the current discrepancy between Primakoff and $e^+e^-$ measurements of the two-photon width of the $\eta$. The Primakoff measurement [27] implies (through (3.22), with $R = 1$) a smaller $\theta_\eta$ than its storage ring counterpart, $\theta_\eta = -7.4 \pm 2.4°$, consistent with the GMO value [10]. Improved measurements of radiative transitions involving the $\eta$ and $\eta'$ mesons would help to constrain the solutions for pseudoscalar mixing angle, and for the inert component of the $\eta'$. In particular, a measurement of $\phi \to \eta'\gamma$ could provide information on the strange quark content of the $\eta'$.

Uncertainties due to strange-quark mass effects can be important in the determination of $\theta_P$. In the scenarios that relate apparent suppressions of radiative decays of strange mesons to a larger mass of the s quark, a significant suppression of the annihilation amplitude of $s\bar{s}$ pairs into two photons is also expected. With the latter suppression of order of 0.5 relative to annihilation amplitudes of non-strange quarks (relevant, e.g., to the model of Ref. [68]), the two-photon widths of both the $\eta$ and $\eta'$ mesons can be described with the standard GMO mixing angle, even if the larger storage ring value of $\Gamma(\eta \to \gamma\gamma)$ is used [111], and no glueball or other "inert" contributions are introduced to their wave functions. The determination of the pseudoscalar mixing angle is clearly model dependent, and a clean-cut choice among various schemes may prove rather difficult to establish.

Experimental indications of a large $\eta-\eta'$ mixing angle stimulated theoretical examination of this mixing from the point of view of a chiral description for ground-state pseudoscalar mesons. A pseudoscalar mixing angle that is larger by about a factor of 2 from that expected on the basis of the GMO quadratic mass formula, seemed to threaten the consistency of the chiral description [112]. However, it was demonstrated from the point of view of the chiral-Lagrangian approach [112], anomalous Ward identities [113] and chiral perturbation theory [114], that there exist quark-mass symmetry-breaking corrections that were not taken into account in the usual formulation. With such $O(m_q^2)$ corrections to both mass matrix and photon decay amplitudes included, a consistent mixing scheme was obtained for such large values of the mixing angle [112, 113, 114].

## 4. Radiative decays of tensor and axial mesons

### 4.1. Experimental situation

For experimental as well as theoretical reasons, radiative decays of tensor and axial mesons have not been studied as thoroughly as those of vectors and pseudoscalars. Experimentally, several radiative decay widths for charged mesons became available for the first time from experiment E272, in particular, $A_2^+ \to \pi^+\gamma$ and $K^{**+} \to K^+\gamma$ in the tensor sector and $A_1^+ \to \pi^+\gamma$ and $B^+ \to \pi^+\gamma$ in the axial sector, all measured using the Primakoff technique. In addition, two-photon decay widths of the $A_2$, f and f' mesons have been measured in $e^+e^-$ storage ring experiments. (Spin-one mesons cannot decay into 2 photons because of Bose statistics for two final photons [115]).

I will begin this Section with a brief discussion of recent results on radiative decays of charged tensor mesons. The Coulombic production of tensor $A_2^+$ and $K^{**+}$ has been

observed through the $A_2^+ \to \pi^+\eta$, $K^+K_S^0$ and $K^{**+} \to K^+\pi^0$, $K_S^0\pi^+$ channels [40]. Using the model for Primakoff production described in Section 2, the following radiative widths have been determined: $\Gamma(A_2^+ \to \pi^+\gamma) = 295\pm60$ keV [40] and $\Gamma(K^{**+} \to K^+\gamma) = 240 \pm45$ keV [48]. As part of the usual procedure, mass, momentum transfer, and decay angular distributions were compared with detailed Monte Carlo simulations, and found to be in good agreement with expectations (cf. Fig. 7 for $A_2^+ \to \pi^+\eta$ distributions). I stress these
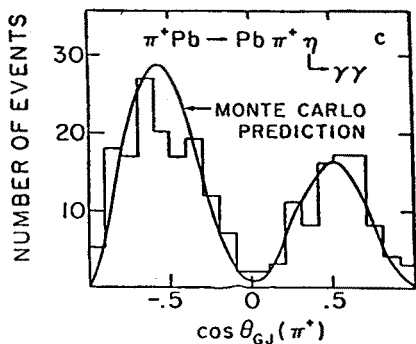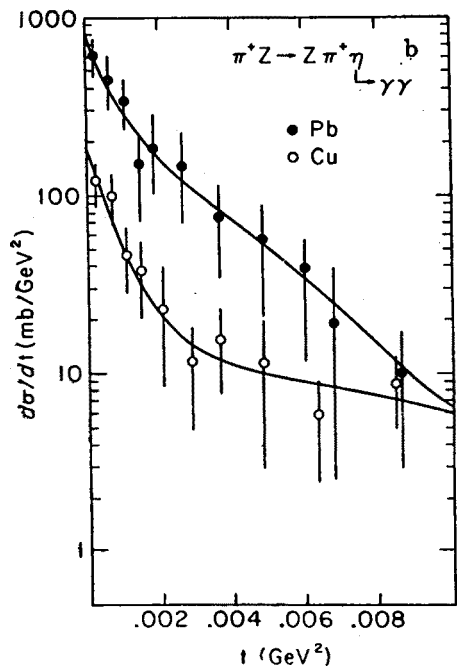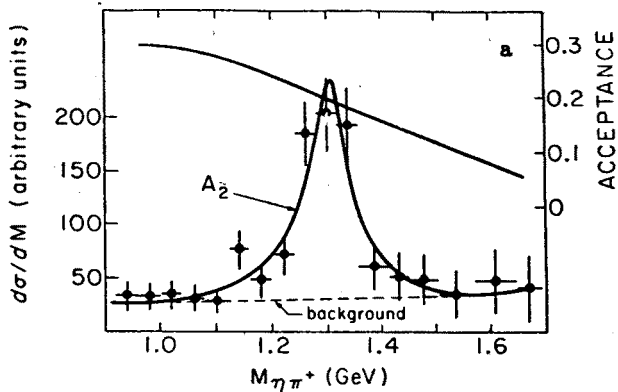


Fig. 7. (a) The mass distributions for $\pi^+\eta$ systems produced coherently on Cu and Pb targets at 200 GeV [40], for $t < 0.01$ GeV$^2$. (b) The $t$-distributions for $A_2$ events with fits of Eq. (2.12) to data. (c) The $\pi^+$ polar angle distribution (in Gottfried-Jackson frame) for $A_2$ events

technical points because these $A_2$ data were used subsequently to check the credibility of a much more complex analysis needed to extract the radiative width of the $A_1$.

The two-photon widths of the $A_2$ and of the f meson have been measured in several $\gamma\gamma$ collision experiments; the two-photon formation of the f' has been observed by the TASSO group [116]. A recent compilation of these results can be found in [10]; the values, averaged over available measurements, are as follows: $\Gamma(f \to \gamma\gamma) = 2.75 \pm 0.14$ keV, $\Gamma(A_2 \to \gamma\gamma) = 1.01 \pm 0.19$ keV and $\Gamma(f' \to \gamma\gamma)B(f' \to K\overline{K}) = 0.11 \pm 0.02 \pm 0.04$ keV. These data are consistent with nonet symmetry for tensor mesons, and a mixing angle $\theta_T$ close to the "ideal" value ($\theta_{ideal} = 35.26°$). Consequently, the f' can be regarded as an almost pure $s\bar{s}$ state.

Now I turn to the discussion of radiative widths of axial mesons: the B(1235) and the $A_1$. Electromagnetic production of the $B^+$ was observed in the $\pi^+\omega$ decay mode [45], and the data are shown in Fig. 8. The Primakoff-extracted radiative decay width of the B is $230 \pm 60$ keV. In addition, the same measurement provided a new determination of the mass and the total width of this meson: $m_B = 1271 \pm 11$ MeV and $\Gamma_B = 232 \pm 29$ MeV. The result of a fit using a relativistic P-wave Breit-Wigner, modified by the coherent production process, plus polynomial terms for the background (dashed line), is shown in Fig. 8 as the full line superimposed on the acceptance-corrected experimental mass distribution. It is clear that these data have very little background to the B signal.

These new values for the mass and width of the B are considerably larger than the standard parameters accepted from earlier measurements [56]. Previous data were obtained in strong-interaction processes that may have been subject to more substantial interference and background effects than those affecting electromagnetic production. Other measurements of masses and widths for the $\varrho^+$, $\varrho^-$, $K^{*+}$, $K^{**+}$ and $A_2^+$ mesons, obtained from the same experiment as the B data, have all agreed with the standard values.

The $A_1$ meson, since its initial observation [117], had eluded an unambiguous analysis of its properties for many years [118]. Only recently have several experiments provided
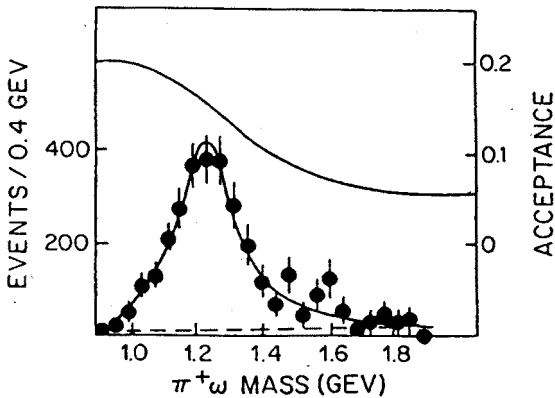


Fig. 8. The mass distribution of $\pi^+\omega$ systems produced coherently on Cu and Pb targets at 200 GeV. The data are clearly dominated by the B(1235). The dashed curve indicates the amount of background required by the fit of Ref. [45]

strong support for a resonant interpretation of the $A_1$; this has been accomplished in studies of diffractive [44, 119, 120], charge exchange [121], baryon exchange [122] and $\tau$-lepton decay [123, 124, 125] processes. Nevertheless, the estimates of the $A_1$ mass and width are still rather uncertain [126]. Therefore, the new high-statistics and high--resolution data on the $A_1$ [44], and, in particular, the evidence for the Coulombic production of the $A_1$, from which the first estimate of its radiative width was extracted [44], have had important impact on the unraveling of the properties of this resonance.

Measuring the radiative width of the $A_1$ is a challenging task. Theoretical estimates of this partial width have been typically of order of 1 MeV. One can therefore expect the Coulombic production of the $A_1$ to be of similar magnitude as that of other mesons discussed previously. In the present case, however, detection of the electromagnetically produced $A_1$'s has to proceed through the only major decay mode known, namely $A_1 \to 3\pi$. The three-pion final states can be also produced coherently on nuclei by strong diffractive processes. In the $A_1$ mass range diffractive production constitutes a background exceeding the anticipated Coulombic process of interest by about an order of magnitude. Nonetheless, extraction of the electromagnetic production of the $A_1$ is possible by isolating the contributions of the relevant angular momentum states to the total $3\pi$ production process by means of a Partial Wave Analysis (PWA). Upon the extraction of such a contribution, the usual Primakoff formalism can be applied to obtain the value of the radiative width.

Since the Primakoff measurement [44] provides the only available experimental information on the radiative width of the $A_1$, and because future refinements of this estimate will most likely have to employ a similar technique, I will discuss the major issues involved in such an analysis. In the following subsection I present relevant information on general features of the $3\pi$ data, on the PWA analysis and, finally, on the extraction of the radiative width: $\Gamma(A_1^+ \to \pi^+\gamma) = 640 \pm 246$ keV [44].

## 4.2. Electromagnetic and diffractive production of the $A_1$

The electromagnetic production of the $A_1$ can be observed, in principle, in interactions of high energy pions with nuclear targets. The main production mechanism of the $A_1$ proceeds, however, through the strong, mostly diffractive, process. Consequently, both the strong and electromagnetic mechanisms have to be discussed together. Because the $A_1$ decays mainly into the $\varrho\pi$ system, its properties have to be extracted from three--pion production data, (2.17), containing also several other sizeable contributions.

The following discussion is based on the author's analysis [42, 43, 44] of measurements by the Rochester–Minnesota–Fermilab collaboration. The data will be compared with the results of other experimental groups, obtained using nuclear as well as proton targets.

GENERAL PROPERTIES OF $3\pi$ PRODUCTION ON NUCLEI

Reaction (2.17), and other similar simple dissociation processes, have over the years attracted considerable experimental and theoretical attention. Two major physics motivations responsible for this continuing interest have been the search for the $A_1$ meson, and studies of inelastic diffraction as a source of information about the propagation of hadronic states through nuclear matter.

Diffractive production of three-pion systems is dominated by a nonresonant Deck component [127]. As a consequence, no resonant peaks (either $A_1$ or $A_2$) can be seen directly in the experimental $3\pi$ mass distributions (cf. Fig. 9).

Similarly, even at an energy of 200 GeV, the momentum transfer distributions for $3\pi$ production (Fig. 10) do not provide much evidence for electromagnetic contributions, that are usually characterized by a forward peak that is much steeper than the slopes of nuclear form factors. Instead, the data exhibit a dip-bump structure, and scaling properties characteristic of nuclear diffraction. The momentum transfer distributions for $0.8 < m_{3\pi} < 1.5$ GeV are shown in Fig. 10 in terms of scaled quantities $\Sigma = \dfrac{d\sigma}{dt}\left(\dfrac{A_{Pb}}{A}\right)^{4/3}$ and $\tau = t\left(\dfrac{A}{A_{Pb}}\right)^{2/3}$. This scaling is suggested for diffractive production by optical models in which diffraction has a geometrical origin [128], and the dominant scale parameter is the nuclear radius $R \sim A^{1/3}$. An approximate universality in $\Sigma$ as a function of $\tau$ is obeyed by the data.

Under closer scrutiny, however, the $t$-distributions for $t < 0.002$ GeV$^2$ appear steeper than at larger $t$-values [129]. The sharpening of the momentum transfer distribution at very small $t$-values can be attributed to a contribution from Coulomb production. Its size
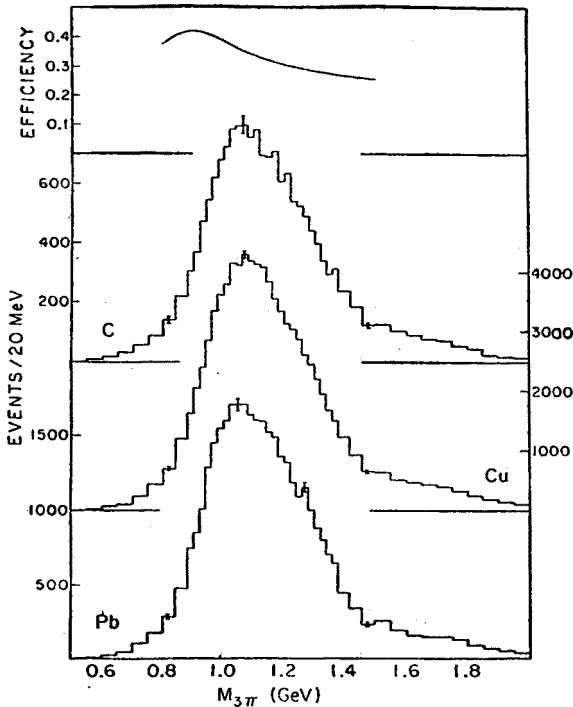


Fig. 9. Mass distributions of $\pi^+\pi^+\pi^-$ systems produced coherently on C, Cu, Pb targets by a 200 GeV $\pi^+$ beam [42]. The data were not corrected by acceptance (detection efficiency, for a limited mass range, is shown at the top)

was estimated in a simple two-component model that included the Coulomb cross-section (calculated using the Primakoff formulae) and an exponential term, representing a strong contribution. The resulting estimate of the Coulomb part was 1.2±0.1 mb on Pb target; a cross-section of 0.32±0.03 mb can be attributed to the production of the $A_2$ resonance [40]. Ascribing the remaining part of the estimated Coulomb cross-section to the production of the $A_1$ state, an estimate for its radiative width was obtained in the range 500–1000 keV [129].

A more reliable separation of Coulomb and diffractive contributions can be achieved by means of a PWA. It has been learned from several PWA's of nuclear $3\pi$ production that the diffractive mechanism favours production of helicity $M = 0$ states in the $t$-channel, particularly at small values of momentum transfers. Coulomb production, on the other hand, involves $M = 1$ states, which carry the helicity of the mediating ($q^2 \approx 0$) photon.

Before proceeding to a discussion of the results of the PWA, I comment briefly on the $A$-dependence of the nuclear $3\pi$ production, which can serve as another indicator of the production mechanism. The Coulomb component, constituting only an estimated 8% of the total integrated coherent cross-section on Pb at 200 GeV, does not visibly affect
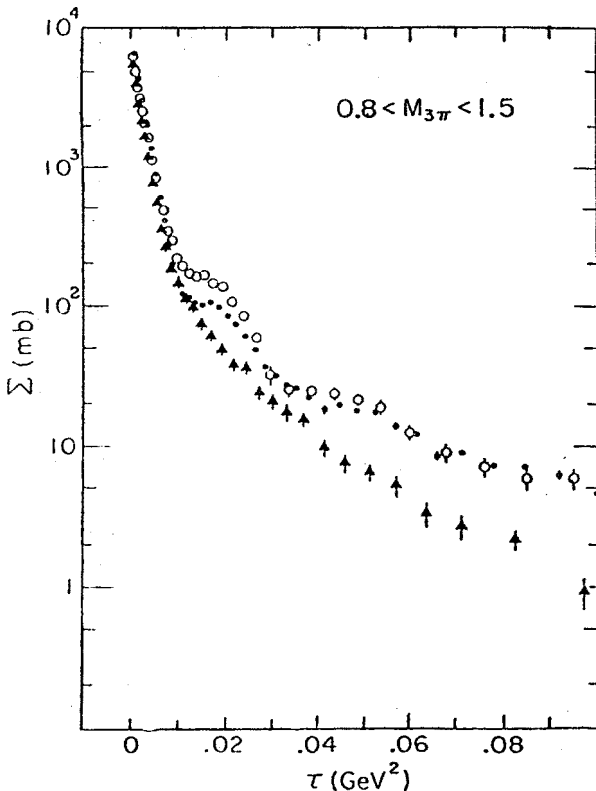


Fig. 10. The geometrically scaled cross-sections (see text for details) for coherent production of $\pi^+\pi^+\pi^-$ systems on C (triangles), Cu (filled circles), and Pb (open circles) at 200 GeV [42]
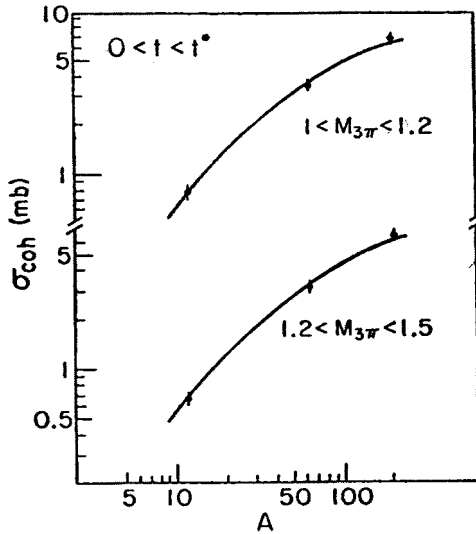
Fig. 11. *A*-dependence of the cross-section for coherent $\pi^+\pi^+\pi^-$ production on nuclei at 200 GeV [42], together with the shape expected from the Kolbig-Margolis model for $\sigma_2 = 15$ mb

the nuclear target dependence of the cross-section. The measurement at 200 GeV [42], Fig. 11, is consistent with both lower energy data [120] and optical model results [130]. This dependence has traditionally been analysed in terms of the Kolbig-Margolis model [131] to extract the total cross-section, $\sigma_2$, of new-born $3\pi$ systems on nucleons, as they propagate through the nucleus. When analysed in terms of this model, the nuclear production data are consistent with the value $\sigma_2 \approx 15$ mb [42, 120]. Similar *A*-dependence has been observed for production of low mass $K^+\omega$ systems by 200 GeV kaons [49]. One should note, however, that the applicability of the model [131], and the interpretation of the parameter $\sigma_2$ as the physical cross-section for unstable hadronic systems, have been questioned by many authors and a variety of alternative approaches to analysing diffractive processes have been proposed [132].

The production of the low-mass $K\omega$ systems, mentioned above, is known to be dominated by the Q mesons [133]. Unlike for the case of the $A_1$, no contribution of electromagnetic production of $K^+\omega$ systems was detected in the E272 data [49]; this was due to much lower event-statistics and more serious acceptance problems. Although only an upper limit $\Gamma(Q \to K\gamma) < 500$ keV could be inferred [134], the radiative width of the Q should be measurable by methods described in this paper.

#### DIFFRACTIVE PRODUCTION OF THE A₁

Many angular momentum states can contribute to the production of $3\pi$ systems in reaction (2.17). The determinations of properties of the $A_1$ meson from such measurements rely primarily on a PWA for separating different spin-parity components, their intensities and relative phases, as functions of $3\pi$ mass and momentum transfer. Most of the recent PWA's of $3\pi$ production (e.g. [43, 119, 120, 135]) employed the Illinois version of PWA, pioneered by Ascoli and collaborators [136]. In such a PWA, the production of $3\pi$ systems

is approximated through an isobar prescription; i.e. it is assumed that the system has a given mass $m$, spin $J$, parity $P'$ and spin projection $M$, and is composed of a single pion and a dipion isobar, with relative angular momentum $L$ (extensive discussion of this approach can be found e.g. in [119, 135, 137]). For low-mass three-pion systems, relevant to the discussion of the $A_1$, a good approximation of the data can be obtained with only a few isobars; usually the $0^+$, $1^-$ and $2^+$ $\varepsilon(770)$, $\varrho(770)$ and $f(1273)$ are used. The contributions of different angular momentum states to the data are described by a density matrix $\varrho_{\alpha\alpha'}$, where the indices $\alpha$, $\alpha'$ represent sets of angular momentum quantum numbers $J^P L M^\eta$. The reflection parity $\eta$ coincides, in the high energy limit, with the naturality of the exchange producing the $3\pi$ system. The density matrix elements $\varrho_{\alpha\alpha'}$ can be extracted from maximum-likelihood fits of a selected set of waves to the data.

The results of three of the most recent experiments [43, 119, 120] for the wave $1^+S0^+(\varrho\pi)$ ($A_1$ quantum numbers) are collected in Fig. 12; the intensity distributions and the phase relative to a $0^-P0^+$ reference wave are displayed as functions of $3\pi$ mass. All three sets of data, although obtained at different energies and on different targets, are in remarkable agreement. In particular, they exhibit strong phase motion of the $1^+S$ wave, which indicates a significant resonant contribution. An additional comment may be in order here. Because only phase differences are measured in a PWA, phase motion of a reference wave can affect the interpretation of the results, especially in the case of broad structures. The least ambiguous measurement of the phase behaviour of the $1^+S0^+$ wave was obtained in Ref. [119] on a proton target, where the $2^+D1^+$ state could be used



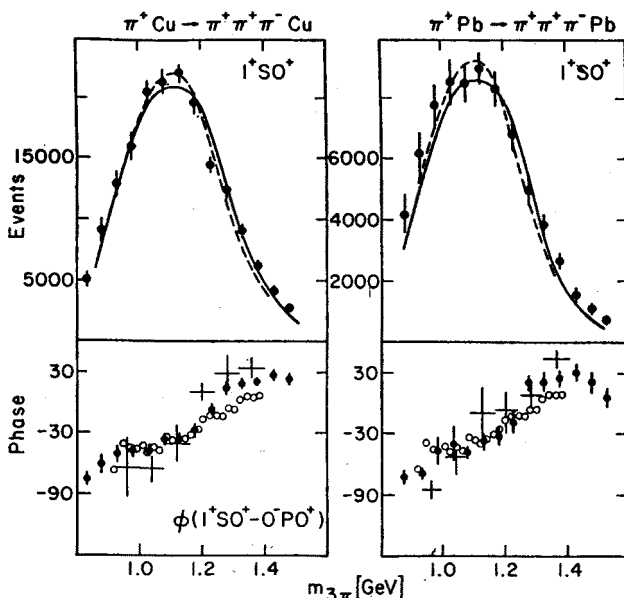Fig. 12. The $1^+S0^+$ wave intensity and its phase relative to $0^-P0^+$ extracted [43] from data on coherent production of $\pi^+\pi^+\pi^-$ systems at 200 GeV (data points). The solid (dashed) lines represent results of fits to the data of Ref. [119] ([120]), normalized to the data points shown. Also displayed are the actual data of [119] (open circles), and [120] (pluses) for the $1^+S - 0^-P$ phase difference

as a reference wave. Because this wave is, practically, saturated by the $A_2$ resonance, its phase is known and the phase behaviour of other waves could be gauged against it. It was established [119] that the 0−P phase had little variation across the $A_1$ bump, while the 1+S wave had substantial phase motion. Since in the nuclear production experiments [43, 120] the $A_2$ signal was too weak to serve as a reference wave, the 0−P wave had to be used for this purpose. According to Ref. [119], the 0−P phase starts to increase above 1.4 GeV and, consequently, the actual motion of the 1+S phase may be even larger than that measured relative to 0−P.

The mass dependence of the 1+S0+ intensity for the most recent measurement of Ref. [43] is represented by the data points in Fig. 12; for clarity, the results of Refs [119] and [120] are displayed as full and broken curves, respectively. The curves were obtained by fitting the data to a two-component unitarity-corrected model of Bowler et al. [138], which includes both direct resonance production and nonresonant Deck background, and takes into account final state rescattering effects. In order to adequately describe the 1+S intensities and phases the fits require significant contributions of a resonant $A_1$; the required $A_1$ mass is in the range of 1.22–1.28 GeV, and the width is about 300 MeV [119, 120, 139].

The above values for the $A_1$ parameters are in disagreement with determinations that use $\tau \rightarrow 3\pi\nu_\tau$ decays. For example, two recent $\tau$ measurements have reported $m_{A_1} = 1056 \pm 25$ MeV and $\Gamma_{A_1} = 476 \pm 143$ MeV [124], and $m_{A_1} = 1194 \pm 14 \pm 10$ MeV and $\Gamma_{A_1} = 462 \pm 56 \pm 30$ MeV [125]. The discrepancy between the two $\tau$ results is due mainly to differences in the parametrizations, not in the actual data; according to the analysis of Ref. [125] the data can sustain a significant contribution from nonresonant $\varrho\pi$.

For consistency, in the following discussion of the electromagnetic production of the $A_1$, I adopt the resonance parameters obtained in analyses of the same source reaction (2.17).

### ELECTROMAGNETIC PRODUCTION OF THE A₁

Evidence for the electromagnetic production of the $A_1$ is provided by the PWA of reaction (2.17) in Ref. [44]. This contribution was identified with the 1+S1+ wave, which had $t$-channel helicity $M = 1$ and exchange naturality $\eta = +$, consistent with photon exchange. The 2+D1+ wave, which is dominated by the $A_2$ meson, was also observed in the analysis of Ref. [44]. Both waves contributed to the total $3\pi$ intensity at a several percent level. Coulomb production of the $A_2$ was also measured in the same experiment, in the clean $\pi^+\eta$ and $K^+K_S^0$ decay modes [40]. Comparison of the latter $A_2$ measurements with the results of the PWA constitutes a crucial test of the sensitivity of the analysis of Ref. [44] to the rather small signals.

Following Ref. [44], I present in Fig. 13 the results of such a comparison for the mass dependence of the 2+D1+ wave intensity and its phase, relative to the 0−P wave. The data points were obtained through a PWA of reaction (2.17). The continuous curves represent the absolute yield of the $A_2$ observed in the cleaner $A_2$ decay channels [40]; dashed curves show the Coulombic yield of the $A_2$ expected from the measured radiative width of the $A_2$, ignoring the contribution from strong production. Considering the difference in the background, the agreement for both targets is surprisingly good. The phase motion of the 2+D1+

wave relative to 0−P was also recovered, and is consistent with the measurement of Ref. [119]. The curves represent the phase behaviour expected from a pure relativistic D-wave Breit-Wigner amplitude; the agreement is quite reasonable. (From the already quoted results of Ref. [119] it is known that the corrections for the intrinsic phase motion of the 0−P wave are small over the mass range of interest.)

Finally, the $t$-dependence of the $2^+D1^+$ intensity for $1.2 < m < 1.4$ GeV is shown in Fig. 14 in comparison with the absolutely normalized $A_2$ differential cross-section expected from the measurement of Ref. [40]. The agreement is again quite good. In particular,
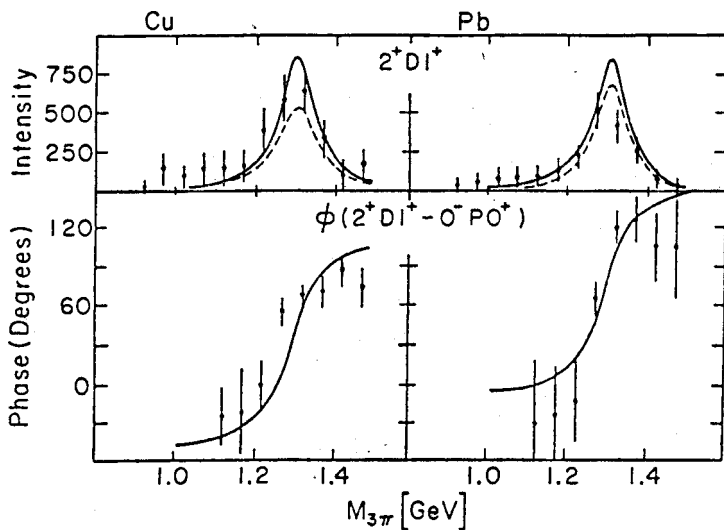


Fig. 13. Intensities and relative phases of $2^+D1^+$ waves extracted [44] from data on coherent production of $\pi^+\pi^+\pi^-$ systems at 200 GeV. Smooth curves are the expectations for $A_2$ production, based on the measurement of Ref. [40]

the $2^+D1^+$ wave does not exhibit the forward dip, characteristic of hadronic spin-flip production observed at lower energies [135]. This result provided strong evidence for Coulombic production of this wave [40, 44]. A very similar $t$-dependence for the spin-flip $1^+S1^+$ wave (candidate for Coulombic production of the $A_1$) is also shown in the same figure.

From a detailed comparison of the $A_2$ signals measured in all the above described processes, one can estimate the overall uncertainty in the intensity of the $2^+D1^+$ wave as about 30%. This same estimate of systematic uncertainty will also be assumed for the $A_1$.

At last, I turn to the discussion of the Coulombic production of the $A_1$. The results of Ref. [44] for the intensities and phases of the $1^+S1^+$ wave, shown in Fig. 15, are consistent with a broad resonance. The curves in the figure correspond to a Primakoff-distorted resonant $A_1$, with parameters of Ref. [119] i.e. $m_{A_1} = 1280 \pm 30$ MeV and $\Gamma_{A_1} = 300 \pm 50$ MeV. The phase variation is somewhat weaker than expected for these parameters, which could be attributed to the presence of a nonresonant contribution or some intrinsic motion of the 0−P reference wave, as indicated in [119]. Although the resonant parameters of the $A_1$ could not be reliably extracted from the measurement of the $1^+S1^+$ wave, it was
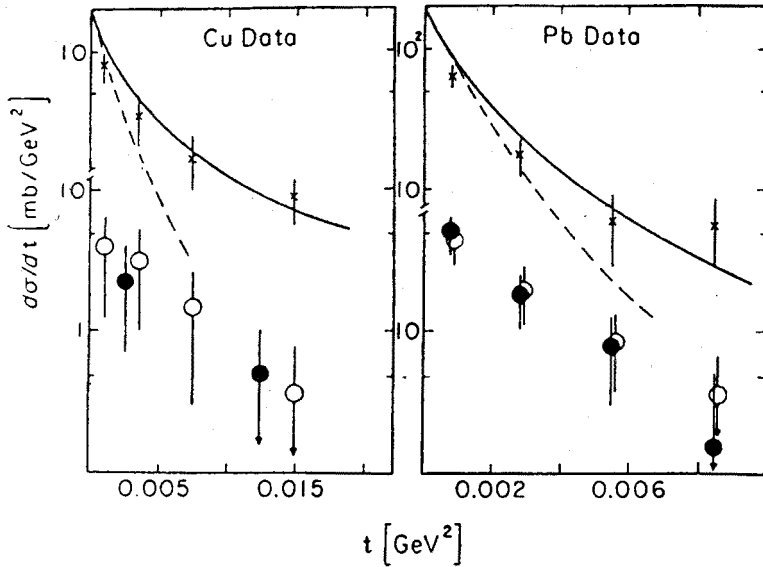
Fig. 14. The $t$-dependence of the $2^+D1^+$ wave (for $1.2 < m < 1.4$ GeV, crosses) and of the $1^+S1^+$ wave (for $1 < m < 1.2$ GeV, open circles, and for $1.2 < m < 1.4$ GeV, solid circles), extracted [44] from data on coherent production of $\pi^+\pi^+\pi^-$ systems at 200 GeV. Smooth curves correspond to the total yield of $A_2$, as observed in [40]; broken curves represent the Coulomb part of the $A_2$ yield
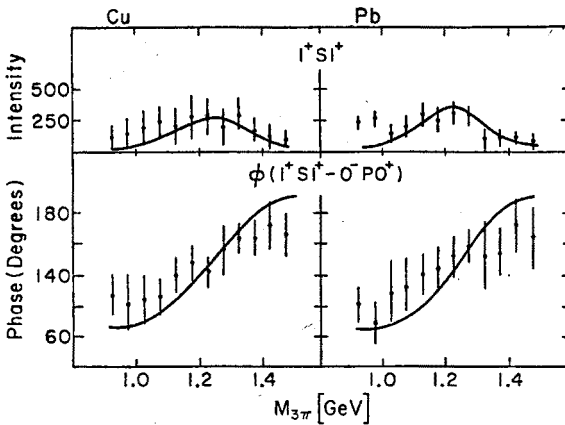


Fig. 15. Intensities and relative phases of the $1^+S1^+$ waves, extracted [44] from data on coherent production of $\pi^+\pi^+\pi^-$ systems at 200 GeV. Smooth curves are predictions based on the standard $A_1$ parameters of Ref. [119]

noted in [44] that an $A_1$ with a mass much below 1.2 GeV would provide a significantly worse description of the data.

To obtain an estimate of the radiative width of the $A_1$, the total intensity for the $1^+1^+$ state, summed over different isobar decay modes, was used in [44]. The $A_1$ is primarily a $\varrho\pi$ $1^+S$ state, nonetheless, the branching ratios to other modes may be not negligible.

Because of the low statistics of the data in the helicity-one channel, the total $1^+1^+$ intensity was calculated assuming the same substructure for the $J^P = 1^+$ state in the $M^\eta = 1^+$ as in the $M^\eta = 0^+$ partial waves. The correction for non-$\varrho\pi$ modes of the $A_1$ resulted in about 20% increase of the radiative width, compared to that using just the $1^+S1^+$ intensity.

The nuclear target dependence can be used as an indication of the production mechanism of the $1^+1^+$ state. The ratio $4.2 \pm 1.0$ of the Pb to Cu cross-sections [44], integrated over $3\pi$ mass range 0.9–1.5 GeV and momentum transfers within coherent forward peaks, is very similar to that measured for the production of the $A_2$ [40], which was demonstrated to occur dominantly in the electromagnetic channel. A deviation from the value of 6.4, expected for pure electromagnetic case, is related in the case of the $A_2$ to interference between Coulomb and hadronic production mechanisms. The quality of the data of Ref. [44] for the $1^+1^+$ wave did not warrant an attempt to separate these two contributions. In the case of the $A_2$, ignoring this interference, would have increased the radiative width by a factor of 1.3.

Using the $A_1$ resonant parameters of Ref. [119], the radiative width of the $A_1$ was quoted as [44] $\Gamma(A_1^+ \to \pi^+\gamma) = 640 \pm 246$ keV. The error includes uncertainties of the maximum-likelihood fits of the PWA, overall normalization error in the experiment (15%), and the estimate of additional systematic uncertainty of 30% (carried over from the study of the electromagnetic $A_2$ production), with all errors added in quadrature.

The result for the radiative width of the $A_1$ is clearly sensitive to the assumed mass and total width. It is interesting to estimate the value of $\Gamma(A_1^+ \to \pi^+\gamma)$ for the $A_1$ resonant parameters obtained from the study of $\tau$ decays in Ref. [124], i.e. for $m_{A_1} = 1056 \pm 25$ MeV and $\Gamma_{A_1} = 476 \pm 143$ MeV. Following the above procedures, and using the data of Ref. [44], a far smaller value of $240 \pm 110$ keV is obtained. Again, the $1^+1^+$ intensity was assumed to be saturated by the $A_1$. The error of 110 keV clearly does not include uncertainties from the choice of the resonant parameters for the $A_1$.

In conclusion, significant evidence for the electromagnetic production of the $A_1$ has been obtained. The extracted estimates of the $A_1$ radiative width fall in the range of values predicted by theoretical calculations. (The theoretical models are reviewed in the next subsection.) With the data improved by an order of magnitude relative to those available in the analysis [44], it should be possible to obtain an accurate measurement of the electromagnetic decay properties of the $A_1$. Such a high statistics measurement would also provide an improved information on other poorly known states contributing to three-pion production, including, in particular, an exotic $J^{PC} = 1^{-+}$ state, which is discussed in Section 5.

## 4.3. Theoretical situation

In terms of multipole decomposition, the tensor and axial meson radiative decays considered in this paper can be viewed as E1 and M2 transitions. There is much less experience with these mesonic transitions than with M1 decays, which have been studied extensively (see the preceding Section). In the treatment of M1 transitions, the quark model, phenomenological Lagrangians and the vector dominance were successfully employed. I discuss below several applications of these ideas to the axial and tensor meson sector.

A multipole analysis of axial and tensor meson radiative decays has been performed by Rosner [82, 140]. This approach is based on a single-quark transition hypothesis for photon and meson emission, as formulated in the work of Melosh [141]. Since several results of Ref. [140] are sensitive to the numerical values of input parameters, which have changed considerably in the past few years, I will now reevaluate the present status of these predictions.

The E1 transition amplitudes are related to $A_1 \to \pi\gamma$ and $B \to \pi\gamma$ decays (the latter involving no quark spin flip), while the M2 component to the $A_2 \to \pi\gamma$. As derived in [140], VDM provides a relation between the E1 and M2 amplitudes. Provided the $\varrho$ meson is dominated by the photon, this relation follows, essentially, from the requirement that the amplitude for the radiative decay of a related isoscalar axial meson $D \to \varrho\gamma$ vanish (again, because the decay of a spin-one state into two identical transversely polarized particles is forbidden by Yang's theorem [115]). In terms of radiative widths, this constraint becomes [140]:

$$[\tilde{\Gamma}(B \to \pi\gamma)]^{1/2} \mp [\tfrac{1}{18} \tilde{\Gamma}(A_1 \to \pi\gamma)]^{1/2} - [\tfrac{5}{54} \tilde{\Gamma}(A_2 \to \pi\gamma)]^{1/2} = 0, \qquad (4.1)$$

where the $\tilde{\Gamma}$'s denote reduced partial widths, with kinematic factors divided out, i.e. $\Gamma = k^3\tilde{\Gamma}$, and $k$ is the decay momentum in the rest frame of the decaying meson. This specific kinematic prescription has been adopted in Ref. [140] as appropriate for single--quark-transitions, but it is obviously model-dependent. For example, in the long-wavelength limit of the nonrelativistic model one expects $2j$-pole radiation to be associated with a kinematic factor of $k^{2j+1}$. It should be also pointed out that a similar $k^3$ momentum dependence was also assumed for hadronic decays of axial and tensor mesons in Refs [82, 140]. On the other hand, models of two-body hadronic transitions often use $k^{2L+1}$ kinematic factors, where $L$ is the relative angular momentum of the decay products. Consequently, predictions of Refs [82, 140] are based on the validity of this particular kinematic prescription, as well as on other physics ingredients of the model (i.e. the single-quark transition hypothesis and VDM).

Relation (4.1) is in approximate agreement with present data only with the choice of the minus sign in the second term; I will consequently assume that form for the ensuing discussion. As a result of this choice, relation (4.1) can be used, e.g., to predict the radiative width of the poorest measured $A_1$ meson. For this one obtains $\Gamma(A_1^+ \to \pi^+\gamma) = 1900 \pm 650$ keV, compared to the experimental value $640 \pm 246$ keV. Relation (4.1) is therefore just barely consistent with the present data. Because of the numerical coefficients in (4.1), the final error is dominated by the error on the radiative width of the B. Note that using the measured widths for the $A_1$ and $A_2$ relation (4.1) could be fulfilled with a value for $\Gamma(B^+ \to \pi^+\gamma)$ about $2\sigma$ below the reported value $230 \pm 60$ keV [45].

With E1 and M2 transition strengths determined by the $A_1$, $A_2$ and B radiative decays, one can calculate the width for $f \to \varrho\gamma$, which includes both (E1) and M2 components. The experimental value for this decay width is not known, but, using VDM, one can relate it to the measured $\Gamma(f \to \gamma\gamma)$. In terms of the reduced widths, one obtains [140]:

$$\tilde{\Gamma}(f \to \varrho\gamma) = 9([\tilde{\Gamma}(B \to \pi\gamma)]^{1/2} + [\tfrac{1}{18} \tilde{\Gamma}(A_1 \to \pi\gamma)]^{1/2})^2 + \tfrac{3}{2} \tilde{\Gamma}(A_2 \to \pi\gamma). \qquad (4.2)$$

Relation (4.1) can be used to eliminate one of the widths on the right-hand side of this equation. Since (4.1) is poorly satisfied by the data, the result for $\Gamma(f \to \varrho\gamma)$ depends on which of the radiative widths remain in the final calculation; the extracted values of $\Gamma(f \to \varrho\gamma)$ range between $0.75 \pm 0.2$ MeV (if the B is eliminated) and $1.6 \pm 0.5$ MeV (if the $A_1$ is eliminated). For the VDM calculation of $\Gamma(f \to \gamma\gamma)$ as indicated in Ref. [140], one obtains the range of $4.1 \pm 1.2$ keV to $8.8 \pm 3.0$ keV (the original estimate of Ref. [140] was $7.7 \pm 2.0$ keV). The result that does not use $\Gamma(B^+ \to \pi^+\gamma)$ is in better agreement with the experimental value of $\Gamma(f \to \gamma\gamma) = 2.65 \pm 0.12$ keV [56]. The calculated value of the two-photon width of the f is somewhat reduced in schemes that consider mixing of this meson with tensor glueball states (see the following Section). In Ref. [142] this reduction factor was estimated to be 0.8–0.9.

Using standard VDM, the $A_1 \to \pi\gamma$, $A_2 \to \pi\gamma$, and $B \to \pi\gamma$ radiative decays can be also related to their decays into a pion and a transversely polarized vector meson ($\varrho$ in case of the $A_1$ and $A_2$, $\omega$ in case of the B):

$$\Gamma(A_{1,2} \to \pi\gamma) = \left(\frac{k_\gamma}{k_\varrho}\right)^3 \frac{\alpha}{\gamma_\varrho^2/\pi} \Gamma(A_{1,2} \to \varrho_T^0\pi), \qquad (4.3)$$

$$\Gamma(B \to \pi\gamma) = \frac{1}{9}\left(\frac{k_\gamma}{k_\omega}\right)^3 \frac{\alpha}{\gamma_\varrho^2/\pi} \Gamma(B \to \omega_T\pi), \qquad (4.4)$$

where an unbroken SU(3) relation between $\varrho\gamma$ and $\omega\gamma$ couplings has been used. If one follows the estimate of Refs [82, 140] for $\gamma_\varrho^2/\pi = 2.7 \pm 0.3$, then the prediction of Ref. [140] for the $A_2$ remains unchanged, $\Gamma(A_2^+ \to \pi^+\gamma) = 375 \pm 50$ keV, and it is consistent with the experimental value.

For the $A_1$ parameters: $m_{A_1} = 1280 \pm 30$ MeV and $\Gamma_{A_1} = 300 \pm 50$ MeV, as determined from diffractive production processes, a result some whatlower than the original estimate is obtained: $\Gamma(A_1^+ \to \pi^+\gamma) = 0.75$–1.4 MeV. This range of values includes uncertainties due to errors on the $A_1$ mass, the total width and the branching into transversely polarized $\varrho$, which depends on $D/S$ decay wave ratio in the $A_1$ decay. The latter branching is $\frac{2}{3}$ if $D = 0$, and about 0.5 if the scale of $D$ is set according to the overall parameters of the single-quark transition hypothesis [140]. The lower end of the predicted range for the radiative width of the $A_1$ is consistent with the measured value. Using, instead, the $A_1$ parameters from $\tau$-lepton decays determined in [124], an expected range of 3–8 MeV is estimated, while the experimental value, as already mentioned, is $240 \pm 110$ keV. I conclude that the $A_1$ parameters obtained from studies of diffractive processes (2.17) are consistent with VDM relations, while those of Ref. [124] are in strong disagreement with experimental data on electromagnetic production of the $A_1$.

The new values for the resonance parameters of the B meson [45] yield a VDM prediction for $\Gamma(B^+ \to \pi^+\gamma)$ of $274 \pm 48$ keV; the result using previous world averages for the B was $184 \pm 30$ keV. Both values are consistent with the measured radiative width of $230 \pm 60$ keV, however, the new VDM result is just barely consistent with constraint (4.1). Considering the sensitivity of relation (4.1) to the radiative width of the B it is likely that

TABLE V

Comparison of experimental data on radiative widths of axial and tensor mesons with several theoretical calculations. All values of the radiative widths are given in keV. Experimental values were taken from [56], unless specified otherwise. Predictions of Ref. [140] reevaluated with more recent values of input parameters are given in parentheses — see text for more details

| Decay | Experiment | Rosner [140] | Godfrey [68] | Singer [147] | Berger [149] |
|---|---|---|---|---|---|
| $B^+ \rightarrow \pi^+\gamma$ | $230 \pm 60$ | $184 \pm 30$ ($274 \pm 48$ [45]) | 397 | | 440 |
| $A_1^+ \rightarrow \pi^+\gamma$ | $640 \pm 246$ | 1000–1600 (700–1400) | 314 | | 240 |
| $A_2^+ \rightarrow \pi^+\gamma$ | $295 \pm 60$ | $375 \pm 50$ | 302 | | 400 |
| $K^{**+} \rightarrow K^+\gamma$ | $240 \pm 45$ | 312 [82] | 230 | | |
| $f \rightarrow \rho\gamma$ | | $1350 \pm 200$ (550–2100) | | 527 [144] | 220 |
| $f \rightarrow \gamma\gamma$ | $2.7 \pm 0.14$ | $7.7 \pm 2$ (3–12) | 3.6 | $2.66 \pm 0.45$ | 2.3 |
| $A_2 \rightarrow \gamma\gamma$ | $0.87 \pm 0.12$ | 1.7–8 [82] | 1.4 | $0.9 \pm 0.36$ | 0.81 |
| $f' \rightarrow \gamma\gamma$ | $0.11 \pm 0.05$ | 0.59–2.8 [82] | 0.6 | $0.14 \pm 0.04/B(f' \rightarrow K\bar{K})$ | 0.19 |
| $\theta \rightarrow \gamma\gamma$ | see text | | | | |

any approximations introduced in the approach of [140] contribute significantly to this discrepancy. The results of Ref. [140] for axial and tensor radiative decays are summarized in Table V, together with available data and relevant predictions of other models.

Certain calculations of tensor radiative decays have predicted very large rates (~10 MeV) for $A_2 \rightarrow \omega\gamma$ and $f \rightarrow \rho\gamma$ decays [143]. Radiative widths of this order imply, through VDM, two-photon widths far larger than have been observed. This has been interpreted as a failure of VDM and of the multipole description for tensor meson decays [144]. Improvement of measurements of axial and tensor meson radiative widths would therefore be of clear importance for evaluating the applicability of these ideas.

The results of the previously discussed QCD-improved quark model of Ref. [68] are also included in Table V. This model reproduces general trends of the data, although the results deviate rather significantly from the measured values in a few cases. It should be noted, however, that the relativistic features inherent in the model are important for achieving the observed level of agreement. A calculation of two-photon decays of tensor mesons in the nonrelativistic "contact" quark annihilation model predicts decay rates that are a factor of 20 too large [111]. Comparing with the results of Ref. [140], differences for radiative widths of the $A_1$ and B are apparent. In particular, the results of Ref. [68] are not in agreement with relation [4.1] of Ref. [140]. The discrepancies between these two approaches can be related to different momentum dependences of the decay amplitudes in the two models, and to the explicit dependence of the calculation in Ref. [68] on the details of meson wave functions, which does not come in the single-quark transition picture [140]. These differences demonstrate the dependence of the predictions on the choice of theoretical models.

An interesting result concerning the $A_1$ meson has been obtained in Refs [89, 90] within the chiral description of axial mesons. It was shown that the longstanding inability of this approach to accommodate the properties of the $A_1$ (as observed in diffractive

processes) can be overcome through a suitable generalization of an effective Lagrangian. A new term has been introduced into the Lagrangian that spoils the Weinberg relation for the $A_1$ mass [145], and provides a simultaneous description of the mass and total width of the $A_1$, and the $\varrho \to \pi\pi$ decay width. Without the new term, the theoretical results for these parameters tend to be significantly lower than the measured values (see e.g. [90] for a discussion of this point). Within the extended scheme, a straightforward application of the VDM provides a prediction for the radiative width of the $A_1$ of 740 keV [89], which agrees with the experimental result. There are, however, significant differences in the implementations of VDM in Refs [89] and [140]; the former uses S-wave decay phase-space (i.e. the decay rate was assumed to be proportional to the first power, rather than the cube, of the decay momentum), and it also neglects any possible interference between the S and D decay waves.

The uncertainties related to applications of the VDM hypothesis were circumvented in the approach of Ref. [146]. In this model, the two-photon and $T \to \gamma V$ decays of the tensor mesons were calculated from a Veneziano-type dual amplitude describing the scattering of pseudoscalar mesons on vector mesons. Using crossing symmetry of the amplitude, and duality, the couplings of tensor mesons, dominating the $s$-channel, have been related to vector contributions to the crossed channels. The $T \to \gamma\gamma$ couplings were expressed by one-photon decay widths of vector mesons and by strong couplings of tensor mesons to two pseudoscalars, without invoking VDM. The calculations of Ref. [146] were updated in [144], after several new measurements of vector-meson radiative widths, needed as an input, became available, and extended in [147] to include f' $\to \gamma\gamma$ decays, which are sensitive to SU(3) breaking. The agreement of the model with the measured values is very good (see Table V). It may be interesting to note that this model [147] relates correctly the symmetry breaking patterns observed in vector and tensor meson radiative decays (very similar results were obtained in [144] using the tensor-dominance model of Renner [148]).

Finally, results of an older calculation [149] of several radiative decays of vector and axial mesons are included in Table V for sake of comparison. The calculation was performed within a nonrelativistic quark-oscillator model. Because the experimental data were not available at that time, the harmonic-oscillator-well width, assumed in derivation of the presented results, was not optimized to fit the data.

## 5. Radiative meson decays and searches for gluonic states

Radiative decays have been used as one of the major tools in searches for novel meson--like states of hadronic matter, that cannot be represented as usual $q\bar{q}$ mesons of the quark model. These still hypothetical new objects include, in particular, glueballs (with wave functions dominated by a pure glue component), hybrid (hermaphrodite, or meikton) mesons (which contain a valence gluon in addition to a $q\bar{q}$ pair in a color-octet state) and multiquark state ($qq\bar{q}\bar{q}$ being the simplest one). The existence of such objects is natural within the general QCD picture of hadrons [150], and it is supported by many specific calculations based on QCD sum rules, lattice simulations, and more phenomenological approaches such as QCD-bag or potential models.

Much effort, both experimental and theoretical, has been devoted to the spectroscopy of glueballs, for which several candidates exist (see, e.g., [151]). It has been also realized, however, that hybrid states may be as amenable to discovery, and perhaps less ambiguous to interpretation. The status of multiquarks states may prove most difficult to evaluate because of their anticipated large widths [152]. Light scalar states have been considered in the literature as candidates for four-quark objects [153]. The electromagnetic properties of the light scalars $\delta(980)$ and $S^*(975)$ have recently been analysed from the point of view of their possible exotic $q\bar{q}q\bar{q}$ assignments in [111, 154, 155].

The interrelation between searches for gluonic states and the electromagnetic properties of hadrons is severalfold. The radiative decays of $J/\psi$ have long been considered a potentially rich source of glueball states. In the QCD framework, $J/\psi$ radiative decays proceed through a two gluon intermediate state (in addition to the photon) [156] and, consequently, enhanced production of gluon-rich final states is expected in such decays. Radiative decays of glueballs are also possible, but only through quark admixtures to their wave functions, thereby providing strong constraints for the interpretations of candidate states. In addition, most of the expected glueballs can mix with normal $q\bar{q}$ mesons, and affect thereby their spectrum and decay properties, including their radiative widths. This property, although obscuring interpretations of glueball candidates, has been used, within various mixing schemes (see, e.g., [9, 15, 104, 106, 157]), to obtain indirect indications of the presence of gluonic states in the spectrum of hadrons. In Section 5.1 I will briefly discuss the phenomenology of glueballs from the point of view of their impact on radiative transitions.

The radiative decays of the hybrid mesons can also serve as a powerful tool for detecting and interpreting such states. The hybrids that are expected to decay into $\pi\gamma$ should also be produced by the Primakoff process, as discussed previously for ordinary mesons. For a given value of the radiative width, the absolute value of the Primakoff production cross-section is uniquely determined. This property can provide strict experimental tests of models that predict $\pi\gamma$ or $\pi V$ couplings of hybrids (VDM can be used in the latter case to estimate the radiative width). The cleanness of the electromagnetic production mode should make it particularly attractive for further experimental searches for such objects. Of special interest in the hybrid sector are exotic states, such as $J^{PC} = 1^{-+}$, with quantum numbers not allowed by the traditional quark models. If discovered, such states would not be subject to ambiguity of interpretation because of possible mixing with $q\bar{q}$ resonances.

Using the electromagnetic mode for searching for hybrid mesons was proposed in Ref. [41]. In Section 5.2 I will elaborate somewhat on this point and discuss the experimental situation.

## 5.1. Radiative decays and glueball spectroscopy

Light glueballs, in the mass range of 1–2 GeV, have been predicted by lattice Monte--Carlo calculations [158], within the MIT bag model [159], and from QCD sum rules [160]. Considering the theoretical uncertainties, the models can provide only qualitative guidance for searches for such states. The leading glueball candidates include the $\iota(1460)$, $G(1590)$,

θ(1710), g(2120), g(2220) and g(2320) [151]. Limited experimental information concerning radiative decays is presently available for the ι(1460) and θ(1710). The following presentation is focused therefore on these two states.

### THE ι(1460)

Since its discovery in radiative J/ψ decays [161], the ι(1460) has been considered a likely glueball candidate. The experimental situation in the ι(1460) mass region is confused due to the presence of at least two states in that mass range, the other established state being the E(1420). Although spin-parity determinations are not yet fully conclusive, $0^{-+}$ assignments are recently favoured for both states [162, 163]. A critical analysis of the available data for the ι/E system is presented in Ref. [164]. New experimental information of the ι(1460) is provided by a low limit on its two-photon decay width [165]:

$$\Gamma(\iota \to \gamma\gamma)B(\iota \to K\overline{K}\pi) < 1.6 \text{ keV} \qquad (5.1)$$

which, together with an estimate $B(\iota \to K\overline{K}\pi) \approx 0.7$, implies $\Gamma(\iota \to \gamma\gamma) < 2.2 \text{ keV}$ (95% C.L.)

The small coupling of the ι(1460) to two photons, and its strong production in the J/ψ radiative decays, intuitively support the glueball interpretation. On the other hand, to explain a large coupling to the $K\overline{K}\pi$ system many models require a significant quark admixture in the ι(1460). In particular, both the small two-photon width and the large hadronic width can be understood assuming that the ι(1460) is predominantly composed of glue and of an electromagnetically inert quark component, $u\overline{u}+d\overline{d}-5s\overline{s}$, which does not couple to two photons [164]. In this picture a small $\varrho\gamma$ and relatively large $\phi\gamma$ decay widths of the ι(1460) are expected. The latter width is presently not known, the former has been estimated from observed J/ψ → γ(ϱγ) decays to be about $1.5 \pm 0.4$ MeV [166, 167]. Using VDM [168], this value implies a much larger two-photon decay width ($\Gamma(\iota \to \gamma\gamma) \approx 11$ keV) than is allowed by the experimental upper limit. It should be noted, however, that, because of significant differences seen in the γϱ and $K\overline{K}\pi$ mass distributions [166, 167], not all of the observed J/ψ → γ(ϱγ) decays may be associated with the ι(1460).

The present limit on the two-photon decay width of the ι(1460) disagrees with several recent calculations based on $\eta - \eta' - \iota$ mixing, which range between 2.5 and 16 keV [169], but is consistent with a QCD sum rules prediction [170], that $\Gamma(\iota \to \gamma\gamma) \approx 1.5 \pm 0.5$ keV. Measurements of ϱγ and φγ decays of the ι(1460), as well as its two-photon width, will be important for testing its interpretation as a glueball, and its mixing with $q\overline{q}$ mesons.

The status of the ι(1460) as a mixture of radial excitations of the pseudoscalar nonet has been reviewed by Lipkin [171]. His approach provides several testable relations between couplings of the ι(1460) and E(1420) to photons and nonstrange hadrons [172], however, the relevant data are not presently available.

### THE θ(1719)

The θ(1710), like the ι(1460), was discovered in the radiative J/ψ decays [173], and for similar reasons has been regarded as a possible glueball candidate, especially because the existence of a gluonic tensor state below the mass of 2 GeV was expected on the basis of several theoretical calculations [174].

The conjecture that the θ(1710) might be a glueball was strengthened by observations of its helicity, that differed markedly from the ones measured for the nearby tensors f and f' [167]. The helicity properties of the J/ψ → γθ amplitude can be understood by regarding the θ(1710) as a 2$^{++}$ glueball, with a small D-wave contribution to the dominant S-wave component of the wave function [175].

Even before the discovery of the θ(1710), SU(3) and SU(6) analyses of the properties of the f meson revealed indications of its possible mixing with a glueball state [142]. The θ(1710) has been examined on this basis, together with the f and f', in a mass matrix analysis in Ref. [9]. After a subsequent development of this model [157], it was believed that such mixing was ruled out by the experimental limit on the two-photon width of the f': $\Gamma(f' \to \gamma\gamma)B(f' \to K\bar{K}) = 0.11 \pm 0.02 \pm 0.04$ keV [176]. (This model required the width to be of order of 10 eV. A version in which the f and θ(1710) mixed together, and the f' remained unmixed, was not ruled out, but appeared unnatural.) This conclusion has recently been contradicted by a very similar f−f'−θ mixing analysis [177]. A mixing matrix solution has been found in [177] that is consistent with the data on f → γγ, f' → γγ, A$_2$ → γγ, J/ψ → ω(f, f') and J/ψ → φ(f, f') decays, and does not contradict the flavour independence of θ(1710) decays that would be expected for a glueball. The two-photon width of the θ(1710) was predicted to be $0.3 \pm 0.1$ keV, to be compared with the experimental limit $\Gamma(\theta \to \gamma\gamma)B(\theta \to K\bar{K}) < 0.28$ keV [178]. Improved measurements of this limit, and of $K\bar{K}$ and ππ decays of the θ(1710) and f', are needed to clarify the situation.

Meanwhile, with f−f'−θ mixing appearing to be ruled out [157], a different scheme has been considered [179] in which the G(1410) took the place of the θ(1710), and no contradiction with experiment was encountered. More recently, a mixing analysis of the tensor masses and decay widths [104] has claimed a lower limit on the glueball mass in this channel of $m > 1880$ MeV. If correct, this result would exclude both the θ(1710) and the G(1410) as glueballs that mix with f and f'.

## 5.2. Radiative decays of hybrid mesons

In the QCD-motivated pursuit of gluonic degrees of freedom in hadron spectroscopy, several hybrid states have been predicted to exist at low masses. Unfortunately, there is very little experimental information available in the literature on such hybrid states [56].

Rather than reviewing the spectroscopy of hybrids, I will concentrate on a particularly interesting exotic $I = 1$, $J^{PC} = 1^{-+}$ state, which will be denoted by $\tilde{\varrho}$. This kind of state is expected on the basis of recent calculations using QCD sum rules [180, 181, 182], QCD bag [183, 184, 185], flux tube [186] or potential [187] models. Although the results of these calculations differ concerning the expected mass ($m$ of 1–2 GeV), width (typically of order of 50–200 MeV), and dominant decay modes (the $\varrho\pi$ branching, in particular, being large in some models [180, 181] and suppressed in others [187]), several of the proposals for $\tilde{\varrho}$ are accessible to experimental study, as discussed below. To put the discussion in perspective, I have collected in Table VI a summary of the theoretical expectations.

Given a relatively large width, and a $\varrho\pi$ decay mode of a hybrid, a strong radiative

TABLE VI

Summary of theoretical expectations for mass, width, and decay modes of $I = 1$, $J^{PC} = 1^{-+}$ exotic hybrid meson ($\tilde{\varrho}$)

| Calculation | $m_{\tilde{\varrho}}$(GeV) | $\Gamma_{\tilde{\varrho}}$(MeV) | Decay modes | Model |
|---|---|---|---|---|
| [180] | ≈1.3 | 20–200 | $\varrho\pi$, $\eta\pi$, $\eta'\pi$, $\pi A_1$, $\pi B$ | QCD sum rules |
| [181] | 1.6–2.1 | 700–2000 | $\varrho\pi$, $\eta\pi$, $\eta'\pi$, K*K | QCD sum rules |
| [182] | ≈1 | | | QCD sum rules |
| [183] | ≈1.4 | | $\eta\pi$, $\pi f$, K*K | QCD bag |
| [184] | 1.4–1.8 | | $\eta\pi$, $\eta'\pi$, $\eta A_1$, K*K, KQ, $\pi B$, $\pi D$ | QCD bag |
| [185] | 1.3–1.6 | 30–80 | $\varrho\pi$, $\eta\pi$, $\eta'\pi$, K*K | QCD bag |
| [186] | 1.6–1.9 | ≈180 | $\pi B$, $\pi D$ | QCD flux tube |
| [187] | ≈2.1 | | $\tilde{\varrho} \to$ PT, PA; $\tilde{\varrho} \nleftrightarrow$ PV, PS | potential |

coupling (to $\pi\gamma$) is also expected. Using the VDM relation

$$\Gamma(\tilde{\varrho}^+ \to \pi^+\gamma) = \frac{\alpha}{\gamma_{\varrho}^2/\pi} \left(\frac{k_\gamma}{k_\varrho}\right)^3 \Gamma(\tilde{\varrho}^+ \to \varrho^0\pi^+) \qquad (5.2)$$

the radiative width of a $\tilde{\varrho}$ can be estimated to be between several hundred keV, for a state predicted in [180] (at mass of 1.3 GeV), and several MeV, for a state at $m_{\tilde{\varrho}} \approx 2$ GeV [181]. A hybrid state with such a large radiative width would be produced at detectable levels through the Primakoff mechanism in coherent interactions of pions with nuclei.

This possibility was first proposed and investigated in [41] using data on coherent $\varrho\pi$ production on nuclei [42, 43] for $m < 1.5$ GeV. The analysis procedures were identical to the ones used in the successful study of the $A_1$ and $A_2$ [44], and have already been outlined in this paper. Note, that for a substantial $\varrho\pi$ decay mode the expected signal from a low mass $\tilde{\varrho}$ is of similar magnitude as that observed for the $A_1$ and $A_2$.

The angular momentum state relevant to the $\tilde{\varrho}$, the $1^-P1^+$ wave, was isolated using the PWA that was described before. The corresponding mass and momentum transfer distributions, Fig. 16, and their $A$-dependence, have been examined for the presence of Coulombic contributions. The data do not exhibit any significant narrow structure in mass, and the $t$-distributions are not peaked nearly as sharply in the forward direction as expected for dominant electromagnetic production. This clearly indicates that a large contribution from non-Coulombic background must be included in order to account for the data.

Assuming different values of the $\tilde{\varrho}$ mass and total width, the four spectra shown in Fig. 16 were fitted for a $\tilde{\varrho}$ radiative width and strong background (two parameters). The same optical model [30] was used here as in the extraction of the radiative widths of the other mesons discussed previously. A typical result is also shown in Fig. 16: for a $\tilde{\varrho}$ mass of 1.25 GeV and width of 50 MeV a radiative width of $\Gamma(\tilde{\varrho}^+ \to \pi^+\gamma)B(\tilde{\varrho}^+ \to \varrho^0\pi^+)$ = 15±8 keV was obtained.

The results for the fitted radiative widths are summarized in Fig. 17, for several values of total width, as a function of assumed resonance mass of the hybrid $\tilde{\varrho}$. The lines in the
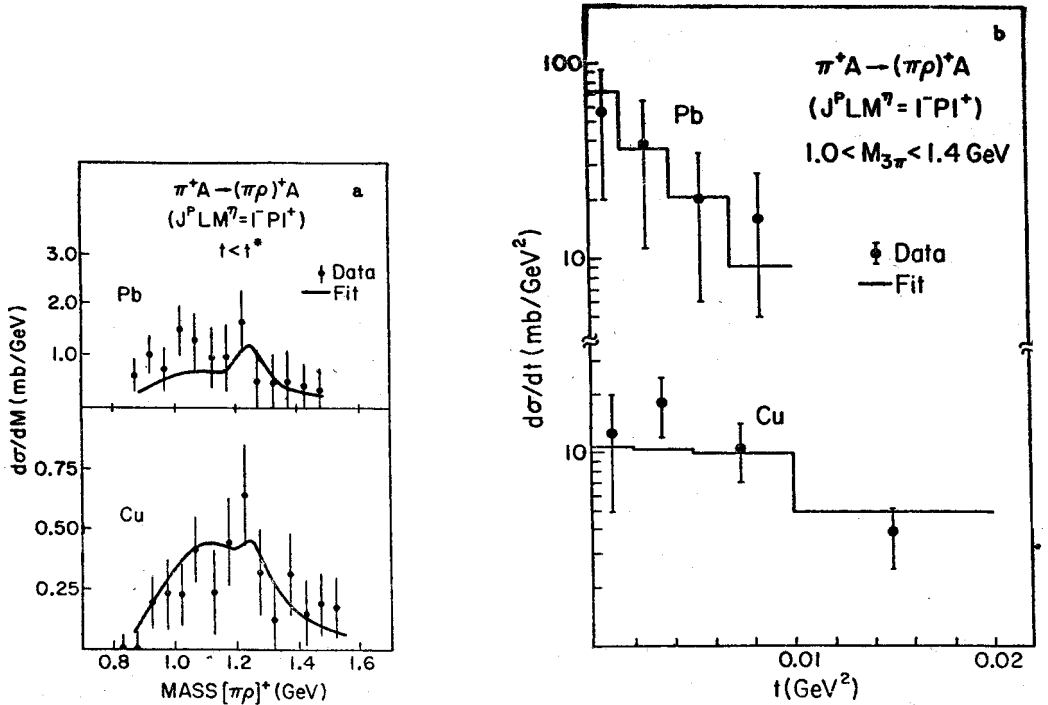
Fig. 16. (a) Mass and (b) $t$-dependences of the $1^- \mathrm{P} 1^+$ intensity, extracted from data on coherent production $\pi^+ \pi^+ \pi^-$ systems at 200 GeV, together with the result of a typical fit assuming $m_{\tilde{\varrho}} = 1.25$ GeV, $\Gamma_{\tilde{\varrho}} = 50$ MeV, and a fitted value of $\Gamma(\tilde{\varrho}^+ \rightarrow \pi^+ \gamma) B(\tilde{\varrho}^+ \rightarrow \varrho^0 \pi^+) = 15 \pm 8$ keV [41]

figure indicate the upper edges of one standard deviation bands for $\Gamma(\tilde{\varrho}^+ \rightarrow \pi^+ \gamma) B(\tilde{\varrho}^+ \rightarrow \varrho^0 \pi^+)$. The errors include the uncertainties of the PWA maximum likelihood fits, and the estimated 30% overall normalization uncertainty, that was carried over from studies of the $A_1$ and $A_2$.

From Fig. 17 it is apparent that the size of resonant $\tilde{\varrho}$ signal that can be accomodated by the data is a factor of $\approx 10$ smaller than expected if the $\tilde{\varrho}$ decayed primarily into $\varrho \pi$, that is, if $B(\tilde{\varrho}^+ \rightarrow \varrho^0 \pi^+) \approx 0.5$. The VDM estimate of the expected ratio of the widths into $\varrho^0 \pi^+$ and $\pi^+ \gamma$ for a $1^-$ state is $\approx 100$ at a mass of 1.3 GeV. Analogous VDM predictions for the $A_2$ and $A_1$ mesons are approximately satisfied by the data.

Fig. 18 presents a comparison of expected and observed radiative width of the $\tilde{\varrho}$, as a function of its width, for a representative resonance mass of 1.3 GeV (as predicted in [180]), and assuming $B(\tilde{\varrho}^+ \rightarrow \varrho^0 \pi^+) \approx 0.5$. It is clear that the observed level of Coulomb production of the hybrid is inconsistent with expectation, except perhaps for very narrow total widths of $<15$ MeV. The conclusion from the presented analysis is that the data do not support the existence of a $J^{PC} = 1^{-+}$ resonant object with a mass below 1.5 GeV and a width larger than 20 MeV, that couples dominantly to $\varrho \pi$.

The discrepancy between the VDM prediction and the observed level of the signal can be avoided if the branching $B(\tilde{\varrho}^+ \rightarrow \varrho^0 \pi^+)$ is sufficiently small. The requirement that
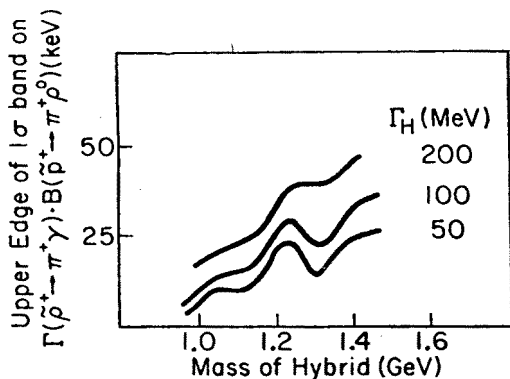
Fig. 17. The upper edges of 1 standard deviation bands on the fitted value of $\Gamma(\tilde{\rho}^+ \to \pi^+\gamma)B(\tilde{\rho}^+ \to \rho^0\pi^+)$, as function of $m_{\tilde{\rho}}$, for several values of the total width of the hybrid state $\tilde{\rho}$ [41]
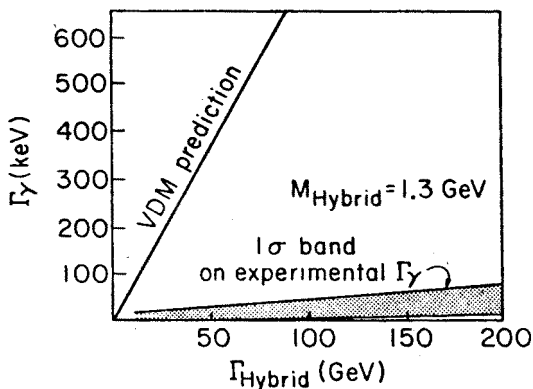


Fig. 18. Comparison of the VDM prediction, Eq. (5.2), and the experimental values of $\Gamma(\tilde{\rho}^+ \to \pi^+\gamma)$, extracted under assumption that $B(\tilde{\rho}^+ \to \rho^0\pi^+) \approx 0.5$, as a function of $\Gamma_{\tilde{\rho}}$, at a representative mass of 1.3 GeV [41]

the VDM prediction be satisfied can be translated [41] into an upper limit on $B(\tilde{\varrho}^+ \to \varrho^0\pi^+)$ $\lesssim 0.2$. This result suggests that other channels of the $\tilde{\varrho}$ must be dominant if such a state exists below $\approx 1.5$ GeV. An analysis of low mass $\eta\pi$ systems [41], proposed as another likely decay mode of the $\tilde{\varrho}$ [180, 183, 184, 185] provided an even more stringent limit for the $\tilde{\varrho}$. As presented already in Section 4.1, the $\eta\pi$ data [40] are dominated by Coulomb production of the $A_2$ (cf. Fig. 7). A particularly strong constraint on the contribution from a $1^-$ resonance is provided by the angular distribution of the $\pi^+$, which is clearly dominated by the D-wave decay of the $A_2$. The P-wave decay distribution of the $\tilde{\varrho}$ should have a maximum, instead of the observed minimum, at $\cos\theta \approx 0$. (The full curves in Fig. 7 represent distributions expected only from the $A_2$.) As a consequence, a rather low limit has been obtained for $\Gamma(\tilde{\varrho}^+ \to \pi^+\gamma)B(\tilde{\varrho}^+ \to \varrho^0\pi^+) \lesssim 0.03$ [41].

The original study [41], and the present discussion, demonstrate the usefulness and sensitivity of Primakoff production in searching for states that couple to $\varrho\pi$. With about

ten times the data that was available for the above analysis one should be able to conduct a more conclusive search for the hybrid $\tilde{\varrho}$ for a range of parameters that would cover most of the predictions, i.e. for $\varrho\pi$ widths as low as about 10 MeV and/or mass values of up to about 2 GeV.

## 6. Summary

Throughout the preceding discussion, I tried to illustrate the diversity and the richness of physics in the study of radiative decays of mesons. This great breadth makes it all the more difficult to provide a coherent and concise summary. I will recapitulate these topics that, in my opinion, are of most interest for future work.

Recent accurate measurements of radiative widths of several mesons have made it possible to quantitatively test old ideas on the quark model, symmetry relationships and vector meson dominance. In general, new implementations of these approaches do quite well in describing the data. The following physics issues have become more fully clarified as a result of this reanalysis process.

● Relativistic properties of light quark systems appear to have a profound influence on the observed level of electromagnetic transition rates. Detailed investigations of such relativistic effects have just begun within QCD-based dynamical models, and more phenomenological approaches, such as harmonic-oscillator quark models. Initial work has achieved significant success in explaining major patterns of the data, and further refinement is therefore of clear interest.

● Quark mass effects have been found important, but are not yet fully understood. The recently determined precision widths for $K^{*+} \to K^+\gamma$, $K^{*0} \to K^0\gamma$, $\phi \to \pi^0\gamma$, and $\phi \to \eta\gamma$ decays, are sensitive to such effects. Their better understanding is of particular importance for evaluating different mixing schemes and for addressing the question of gluonic content of conventional mesons. In general, electromagnetic decays provide a sensitive measure of symmetry breaking effects.

● As an unforeseen development, new data on radiative decays of light mesons have proved useful for phenomenological tests of recent extensions of low-energy chiral Lagrangians that are important for soliton models of baryons.

● Experimentally, the Primakoff technique and photon-photon collisions in $e^+e^-$ interactions have emerged as major tools for measurements of radiative widths at high energies. Several independent tests of the Primakoff formalism have demonstrated the method to be fully reliable.

● Resolving the present discrepancy between the Primakoff and $e^+e^-$ measurements of the $\eta \to \gamma\gamma$ width is important for understanding mixing effects in the pseudoscalar sector. A measurement of $\phi \to \eta'\gamma$ would also aid such a study, by constraining the strange quark content in the $\eta'$. Strong indications of gluonic admixtures to the $\eta'$ wave function have already been inferred from available data.

● With the $\varrho^+ \to \pi^+\gamma$ decay width now accurately known, it becomes even more crucial to remeasure the $\omega \to \pi^0\gamma$ process and solve the longstanding controversy concerning the value of the radiative width of the $\omega$. The value of the ratio of radiative widths of the

$\varrho$ and $\omega$ is an essential parameter in most models of electromagnetic decays of vector and pseudoscalar mesons.

- An improved measurement of the electromagnetic production of the $A_1$ is of interest, not only for precision determinations of E1 and M2 multipole amplitudes, but also because this would add a decisive argument to current disputes concerning the mass and width of this meson.

- Electromagnetic interactions may be as important for potential discoveries of novel states of hadronic matter as they are for unraveling the structure of conventional mesons. Improved measurements of two-photon widths of the $\iota(1460)$ and $\theta(1710)$ would help clarify their interpretations as glueball states. The Primakoff method has been recognized as a sensitive way of searching for certain exotic hybrid states. First results are promising enough to encourage further effort in this interesting field.

In conclusion, significant progress has been achieved in studies of electromagnetic properties of mesons over the past few years. In many areas the work has just started and is progressing at fast pace. Many fundamental properties of bound states of light quarks have been scrutinized in studies of radiative decays. Further experimental and theoretical effort in this field will certainly have important impact on our understanding of large-scale properties of hadrons.

## REFERENCES

[1] M. Gell-Mann, *Phys. Lett.* **8**, 214 (1964); G. Zweig, CERN report 8419/TH (1964); J. J. Kokkedee, *The Quark Model*, W. A. Benjamin, Inc., New York 1969; A. W. Hardy, D. B. Lichtenberg, *Rep. Prog. Phys.* **41**, 1707 (1978); F. E. Close, *An Introduction to Quarks and Partons*, Academic, London 1979.

[2] F. Gursey, L. A. Radicati, *Phys. Rev. Lett.* **13**, 173 (1964); B. Sakita, *Phys. Rev.* **136**, 1756B (1964); G. Grunberg, F. M. Renard, *Nuovo Cimento* **33**, 617 (1976).

[3] B. T. Feld, *Models of Elementary Particles*, Blaisdell, Waltham 1969.

[4] M. Gell-Mann, F. Zachariasen, *Phys. Rev.* **124**, 953 (1961); Y. Nambu, J. J. Sakurai, *Phys. Rev. Lett.* **8**, 79 (1962); M. Gell-Mann, D. Sharp, W. G. Wagner, *Phys. Rev. Lett.* **8**, 261 (1962); R. F. Dashen, D. Sharp, *Phys. Rev.* **133**, 1585B (1964); N. M. Kroll, T. D. Lee, B. Zumino, *Phys. Rev.* **157**, 1376 (1967).

[5] R. P. Feynman, *Photon-Hadron Interactions*, Benjamin, New York 1972.

[6] M. A. Shifman, A. I. Vainshtein, V. I. Zakharov, *Nucl. Phys.* **B147**, 385, 448 (1979); N. S. Craige, J. Stern, *Phys. Rev.* **D26**, 2430 (1982); P. Pascual, E. de Rafael, *Z. Phys.* **C12**, 127 (1982); N. N. Nikolaev, A. V. Radyushkin, *Phys. Lett.* **110B**, 476 (1982).

[7] A. Chodos et al., *Phys. Rev.* **D9**, 3471 (1974); **D10**, 2599 (1974); T. De Grand et al., *Phys. Rev.* **D12**, 2060 (1975).

[8] A. De Rujula, H. Georgi, S. L. Glashow, *Phys. Rev.* **D12**, 147 (1975).

[9] H. J. Schnitzer, *Nucl. Phys.* **B207**, 131 (1982).

[10] Ch. Berger, W. Wagner, *Phys. Rep.* **146**, 1 (1987),

[11] L. G. Landsberg, *Phys. Rep.* **128**, 301 (1985).

[12] P. J. O'Donnell, *Rev. Mod. Phys.* **53**, 673 (1981).

[13] A. T. Filippov, *Usp. Fiz. Nauk* **137**, 201 (1982).

[14] S. Cooper, Rapporteur talk at the Europhysics Conference on High Energy Physics, Bari, Italy, July 1985 and SLAC-PUB-3819, 1985.

[15] J. L. Rosner, at International Syposium on Lepton and Photon Interactions, Kyoto, Aug. 1985.

[16] H. W. Atherton et al., *Phys. Lett.* **158B**, 81 (1985).

[17] J. Keyne et al., *Phys. Rev.* **D14**, 28 (1976); A. B. Baldin et al., *Yad. Fiz.* **13**, 758 (1971).

[18] J. T. Dahin et al., *Phys. Rev.* **D6**, 2321 (1972).

[19] W. D. Apel et al., *Phys. Lett.* **41B**, 234 (1972).

[20] C. J. Zanfino et al., *Phys. Rev. Lett.* **38**, 930 (1977).

[21] D. E. Andrews et al., *Phys. Rev. Lett.* **38**, 198 (1977).

[22] V. P. Druzhinin et al., *Phys. Lett.* **144B**, 136 (1984); L. M. Kuradze et al., *Pisma Zh. Eksp. Teor. Fiz.* **38**, 306 (1983); G. Cosme et al., *Phys. Lett.* **63B**, 352 (1976); D. Benaksas et al., *Phys. Lett.* **42B**, 511 (1972).

[23] F. Low, *Phys. Rev.* **120**, 582 (1960).

[24] H. Primakoff, *Phys. Rev.* **81**, 899 (1951).

[25] A. Browman et al., *Phys. Rev. Lett.* **33**, 1400 (1974).

[26] V. I. Kryshkin et al., *JETP* **30**, 1037 (1970).

[27] A. Browman et al., *Phys. Rev. Lett.* **32**, 1067 (1974).

[28] M. L. Good, W. D. Walker, *Phys. Rev.* **120**, 1855 (1960); A. Halprin, C. M. Anderson, H. Primakoff, *Phys. Rev.* **152**, 1295 (1966); N. Jurisic, L. Stodolski, *Phys. Rev.* **D3**, 724 (1971); G. Berlad et al., *Ann. Phys.* **75**, 461 (1973); M. Gourdin, *Nucl. Phys.* **B32**, 415 (1971).

[29] I. Pomeranchuk, I. Shmushkevich, *Nucl. Phys.* **23**, 452 (1961); V. N. Gribov et al., *JETP* **14**, 1308 (1962).

[30] G. Fäldt et al., *Nucl. Phys.* **B41**, 125 (1972); G. Fäldt, *Nucl. Phys.* **B43**, 591 (1972); G. Fäldt, *Phys. Rev.* **D2**, 846 (1970).

[31] R. J. Glauber, *Phys. Rev.* **100**, 242 (1955); R. J. Glauber, in *Lectures in Theoretical Physics*, ed. W. E. Brittin et al., Interscience, New York 1959, Vol. I; R. J. Glauber, in *High-Energy Physics and Nuclear Structure*, ed. S. Devons, Plenum, New York 1970.

[32] T. Jensen et al., *Phys. Rev.* **D27**, 26 (1983).

[33] C. Bemporad et al., *Nucl. Phys.* **B51**, 1 (1973).

[34] A. N. Kamal, G. L. Kane, *Phys. Rev. Lett.* **43**, 551 (1979).

[35] T. Ferbel, in Proceedings of the First Workshop on Ultra-Relativistic Nuclear Collisions, Berkeley, 1979, Lawrence Berkeley Laboratory Report LBL-8957.

[36] R. V. Kowalewski et al., *Phys. Rev.* **D29**, 1000 (1984).

[37] M. Zieliński et al., *Phys. Rev.* **D29**, 2633 (1984).

[38] D. Berg et al., *Phys. Rev. Lett.* **44**, 706 (1980).

[39] J. Huston, *Phys. Rev.* **D33**, 3199 (1986).

[40] S. Cihangir et al., *Phys. Lett.* **117B**, 119 (1982).

[41] M. Zieliński et al., Rochester preprint UR 946 and *Z. Phys. C* **31**, 545 (1986); M. Zieliński et al., Rochester preprint UR 966, 1986, to appear in Proceedings of the XXIII International Conference on High Energy Physics, Berkeley, ed. S. Loken, July 1986.

[42] M. Zieliński et al., *Z. Phys.* **C16**, 197 (1983).

[43] M. Zieliński et al., *Phys. Rev.* **D30**, 1855 (1984).

[44] M. Zieliński et al., *Phys. Rev. Lett.* **52**, 1195 (1984).

[45] B. Collick et al., *Phys. Rev. Lett.* **53**, 2374 (1984).

[46] D. Berg et al., *Phys. Lett.* **98B**, 119 (1981).

[47] C. Chandlee et al., *Phys. Rev. Lett.* **51**, 168 (1983).

[48] S. Cihangir, *Phys. Lett.* **117B**, 123 (1982).

[49] M. Zieliński et al., *Phys. Rev.* **D30**, 1107 (1984).

[50] C. Nelson et al., *Nucl. Instrum. Methods* **216**, 381 (1983).

[51] B. Collick, Ph. D. thesis, University of Minnesota 1984, unpublished.

[52] J. D. Bjorken, S. D. Drell, *Relativistic Quantum Mechanics*, McGraw-Hill, New York 1964.

[53] Yu. M. Antipov et al., *Z. Phys.* **C24**, 39 (1984); *Phys. Lett.* **121B**, 445 (1983).

[54] B. Gobbi et al., *Phys. Rev. Lett.* **33**, 1450 (1974); *Phys. Rev. Lett.* **37**, 1439 (1976).

[55] L. Capraro et al., contributed paper to the XXII International Conference on High Energy Physics, Leipzig, July 1984.

[56] Particle Data Group, compilations, *Phys. Lett.* **170B**, (1986).

[57] D. Carlsmith et al., *Phys. Rev. Lett.* **56**, 18 (1986).

[58] W. C. Carithers et al., *Phys. Rev. Lett.* **35**, 349 (1975).

[59] C. Becchi, G. Morpurgo, *Phys. Rev.* **140B**, 687 (1965).

[60] R. Van Royen, V. F. Weiskopf, *Nuovo Cimento* **50A**, 617 (1967); Y. Anisovich et al., *Phys. Lett.* **16**, 194 (1965); W. Thirring, *Phys. Lett.* **16**, 335 (1965); L. Soloviev, *Phys. Lett.* **16**, 345 (1965).

[61] H. J. Lipkin, *Nucl. Phys.* **B241**, 477 (1983); **B214**, 136 (1983); *Phys. Rev.* **D24**, 1437 (1981).

[62] G. Morpurgo, at Bologna Meeting on Frontiers of Physics, Oct. 1983.

[63] N. Isgur, G. Karl, *Phys. Rev.* **D18**, 4187 (1979); *Phys. Lett.* **74B**, 353 (1978); *Phys. Lett.* **72B**, 109 (1977).

[64] R. McClary, N. Byers, *Phys. Rev.* **D28**, 1692 (1983); P. Moxhay, J. L. Rosner, *Phys. Rev.* **D28**, 1132 (1983); H. Grotch, K. J. Sebastian, *Phys. Rev.* **D25**, 2944 (1982).

[65] S. Ono, *Phys. Rev.* **D27**, 1203 (1983); *Acta Phys. Pol.* **B15**, 201 (1984).

[66] A. C. Sharma, *Lett. Nuovo Cimento* **33**, 445 (1982).

[67] N. Isgur, *Phys. Rev. Lett.* **36**, 1262 (1976).

[68] S. Godfrey, N. Isgur, *Phys. Rev.* **D32**, 189 (1985).

[69] S. Capstick, N. Isgur, Toronto preprint UTPT-85-34, 1985.

[70] C. Hayne, N. Isgur, *Phys. Rev.* **D25**, 1944 (1982).

[71] R. P. Feynman, M. Kislinger, F. Ravndall, *Phys. Rev.* **D3**, 2706 (1971).

[72] T. Barnes, *Phys. Lett.* **63B**, 65 (1976).

[73] S. Ishida et al., *Progr. Theor. Phys.* **71**, 806 (1984).

[74] C. P. Singh, P. K. Chatley, *Phys. Rev.* **D26**, 332 (1982).

[75] S. Okubo, *Phys. Lett.* **4**, 14 (1963); *Phys. Lett.* **5**, 165 (1963).

[76] S. L. Glashow, *Phys. Rev. Lett.* **11**, 48 (1963).

[77] K. Tanaka, *Phys. Rev.* **133**, 1509B (1964).

[78] S. Meshkov et al., *Phys. Rev. Lett.* **10**, 361 (1963).

[79] T. Ohshima, *Phys. Rev.* **D22**, 707 (1980).

[80] A. Bramon, F. J. Yndurain, *Phys. Lett.* **80B**, 239 (1979).

[81] R. Verma, *Phys. Rev.* **D22**, 698 (1980).

[82] J. Babcock, J. L. Rosner, *Phys. Rev.* **D14**, 1286 (1976).

[83] P. J. O'Donnell, *Can. J. Phys.* **55**, 1301 (1977).

[84] G. J. Gounaris, *Phys. Lett.* **63B**, 307 (1976).

[85] E. Etim, M. Greco, *Nuovo Cimento* **42**, 124 (1974).

[86] J. S. Bell, L. Jackiw, *Nuovo Cimento* **60A**, 47 (1969).

[87] S. L. Adler, *Phys. Rev.* **177**, 2426 (1969).

[88] S. Gasiorowicz, D. A. Geffen, *Rev. Mod. Phys.* **41**, 531 (1969).

[89] Ö. Kaymakcalan, J. Schechter, *Phys. Rev.* **D31**, 1109 (1985); H. Gomm, Ö. Kaymakcalan, J. Schechter, *Phys. Rev.* **D30**, 2345 (1984); Ö. Kaymakcalan, S. Rajeev, J. Schechter, *Phys. Rev.* **D30**, 594 (1984).

[90] M. F. L. Golterman, N. D. Hari Dass, Amsterdam preprint NIKHEF-H/85-13, ITFA-85 19, 1985.

510

[91] A. N. Ivanov, V. M. Schechter, *Yad. Fiz.* **31**, 530 (1980).

[92] S. L. Adler, *Phys. Rev.* **D4**, 3497 (1971).

[93] M. V. Terentev, *Phys. Lett.* **38B**, 419 (1972).

[94] J. Wess, B. Zumino, *Phys. Lett.* **37B**, 95 (1971).

[95] E. Witten, *Nucl. Phys.* **B223**, 422 (1981).

[96] G. Kramer et al., *Phys. Rev.* **D30**, 89 (1984).

[97] Yu. M. Antipov et al., *Phys. Rev. Lett.* **56**, 796 (1986).

[98] S. R. Amendolia et al., *Phys. Lett.* **155B**, 457 (1985).

[99] T. H. Skyrme, *Proc. R. Soc. London* **A260**, 127 (1961); A. P. Balachandran et al., *Phys. Rev.* **D27**, 1133 (1983); E. Witten, *Nucl. Phys.* **B223**, 433 (1983); G. S. Adkins et al., *Nucl. Phys.* **B228**, 552 (1983).

[100] W. D. Apel et al., *Sov. J. Nucl. Phys.* **30**, 189 (1979); N. R. Stanton et al., *Phys. Lett.* **92B**, 353 (1980).

[101] A. T. Filippov, *Yad. Fiz.* **29**, 1036 (1979).

[102] S. Okubo, K. Jagannathan, *Phys. Rev.* **D15**, 177 (1977).

[103] N. Fuchs, *Phys. Rev.* **D14**, 1912 (1976).

[104] R. Sinha, *Nuovo Cimento* **92A**, 83 (1986).

[105] R. H. Capps, *Phys. Rev.* **D17**, 1862 (1977).

[106] J. L. Rosner, *Phys. Rev.* **D27**, 1101 (1983).

[107] H. J. Lipkin, *Phys. Lett.* **67B**, 65 (1977).

[108] I. Cohen, H. J. Lipkin, *Nucl. Phys.* **B151**, 16 (1979).

[109] M. Frank, P. J. O'Donnell, *Phys. Rev.* **D29**, 921 (1984); **B32**, 1739 (1985); *Phys. Lett.* **144B**, 451 (1984).

[110] R. M. Baltrusaitis et al., *Phys. Rev.* **D32**, 2883 (1985).

[111] T. Barnes, Invited contribution to the VIIth International Workshop on Photon-Photon Collisions, Paris, April 1986.

[112] J. F. Donoghue et al., *Phys. Rev. Lett.* **55**, 2766 (1985).

[113] G. Grunberg, *Phys. Lett.* **168B**, 141 (1986).

[114] J. Gasser, H. Leutwyler, *Nucl. Phys.* **B250**, 465 (1985).

[115] C. N. Yang, *Phys. Rev.* **77**, 242 (1950).

[116] M. Althoff et al., *Phys. Lett.* **121B**, 216 (1983).

[117] G. Goldhaber et al., *Phys. Rev. Lett.* **12**, 336 (1964).

[118] H. E. Haber, G. L. Kane, *Nucl. Phys.* **B129**, 429 (1977).

[119] C. Daum et al., *Phys. Lett.* **89B**, 281 (1980); *Nucl. Phys.* **B182**, 269 (1981).

[120] G. Bellini et al., *Nucl. Phys.* **B199**, 1 (1982); *Phys. Rev. Lett.* **48**, 1697 (1982); *Nuovo Cimento Lett.* **38**, 433 (1983); *Nuovo Cimento* **79A**, 282 (1984).

[121] J. A. Dankowych et al., *Phys. Rev. Lett.* **46**, 580 (1981).

[122] A. Ferrer et al., *Phys. Lett.* **74B**, 287 (1978); B. Foster et al., *Nucl. Phys.* **B187**, 231 (1981).

[123] G. Alexander et al., *Phys. Lett.* **73B**, 99 (1978); J. A. Jaros et al., *Phys. Rev. Lett.* **40**, 1120 (1978); W. Wagner et al., *Z. Phys.* **C3**, 193 (1980).

[124] W. Ruckstuhl et al., *Phys. Rev. Lett.* **56**, 2132 (1986).

[125] W. B. Schmidtke et al., *Phys. Rev. Lett.* **57**, 527 (1986).

[126] J. Turnau, *Acta Phys. Pol.* **B13**, 849 (1982).

[127] R. T. Deck, *Phys. Rev. Lett.* **13**, 169 (1964).

[128] T. T. Chou, C. N. Yang, *Phys. Rev.* **D22**, 610 (1980).

[129] D. Berg et al., Proceedings of AIP Conference on Experimental Meson Spectroscopy, ed. S. J. Lindenbaum, 1983.

[130] T. F. Hoang, *Phys. Rev.* **D31**, 2248 (1985).

[131] K. J. Kolbig, B. Margolis, *Nucl. Phys.* **B6**, 85 (1968).

[132] L. Van Hove, *Nucl. Phys.* **B46**, 75 (1972); G. Fäldt, P. Osland, *Nucl. Phys.* **B97**, 445 (1975); H. Miettinen, J. Pumplin, *Phys. Rev.* **D18**, 1696 (1978); *Phys. Rev. Lett.* **42**, 204 (1979); W. Czyż, M. Zieliński, *Acta Phys. Pol.* **B11**, 615 (1980); G. Bertch et al., *Phys. Rev. Lett.* **47**, 297 (1981).

[133] C. Daum et al., *Nucl. Phys.* **B187**, 1 (1981).
[134] T. Ferbel, *Acta Phys. Pol.* **B12**, 1129 (1981).
[135] J. Pernegr et al., *Nucl. Phys.* **B134**, 436 (1978).
[136] G. Ascoli et al., *Phys. Rev.* **D7**, 669 (1973).
[137] J. D. Hansen et al., *Nucl. Phys.* **B81**, 403 (1974).
[138] M. G. Bowler, *J. Phys. G* **5**, 203 (1979); M. G. Bowler et al., *Nucl. Phys.* **B97**, 227 (1975).
[139] R. Aaron, R. S. Longacre, *Phys. Rev.* **D24**, 1207 (1981).
[140] J. L. Rosner, *Phys. Rev.* **D23**, 1127 (1981); see also J. L. Rosner, in Techniques and Concepts in High-Energy Physics, ed. T. Ferbel, Plenum, New York 1981.
[141] H. J. Melosh, *Phys. Rev.* **D9**, 1095 (1974).
[142] J. L. Rosner, *Phys. Rev.* **D24**, 1347 (1981).
[143] V. Privman, P. Singer, *Phys. Lett.* **91B**, 436 (1980); W. N. Cottingham, I. H. Dunbar, *J. Phys. G* **5**, L155 (1979); J. W. Alcock et al., *Nucl. Phys.* **B145**, 85 (1978).
[144] P. Singer, *Phys. Rev.* **D27**, 2223 (1983).
[145] S. Weinberg, *Phys. Rev. Lett.* **18**, 507 (1967).
[146] N. Levy, P. Singer, S. Toaff, *Phys. Rev.* **D13**, 2662 (1976).
[147] P. Singer, *Phys. Lett.* **124B**, 531 (1983).
[148] B. Renner, *Nucl. Phys.* **B30**, 634 (1971).
[149] S. B. Berger, B. T. Feld, *Phys. Rev.* **D8**, 3875 (1973).
[150] H. Fritzsch, P. Minkowski, *Nuovo Cimento* **30A**, 393 (1975); P. G. O. Freund, Y. Nambu, *Phys. Rev. Lett.* **34**, 1645 (1975); J. Kogut, D. Sinclair, L. Susskind, *Nucl. Phys.* **B114**, 199 (1976); D. Robson, *Nucl. Phys.* **B130**, 328 (1977); P. Roy, T. Walsh, *Nucl. Phys.* **B140**, 449 (1978).
[151] S. J. Lindenbaum, *Comments Nucl. Part. Phys.* **13**, 285 (1984); Summer Workshop in High Energy Physics and Cosmology, Trieste, July 1985 and Brookhaven preprint BNL 37412; S. S. Gernstein et al., *Z. Phys.* **C24**, 305 (1984).
[152] R. L. Jaffe, *Phys. Rev.* **D15**, 267, 281 (1977).
[153] N. N. Achasov et al., *Z. Phys.* **C16**, 55 (1983); J. Weinstein, N. Isgur, *Phys. Rev.* **D27**, 588 (1983); A. Bramon, E. Masso, *Phys. Lett.* **120B**, 240 (1983).
[154] T. Barnes, *Phys. Lett.* **165B**, 434 (1985).
[155] S. Narison, Trieste preprint IC/86/12, 1986.
[156] T. Appelquist et al., *Phys. Rev. Lett.* **34**, 365 (1975); M. Chanowitz, *Phys. Rev.* **D12**, 918 (1975); S. Brodsky et al., *Phys. Lett.* **73B**, 203 (1978).
[157] J. L. Rosner, S. F. Tuan, *Phys. Rev.* **D27**, 1544 (1983).
[158] B. Berg, A. B. Moire, *Phys. Lett.* **113B**, 65 (1982); **114B**, 324 (1982); *Nucl. Phys.* **B221**, 109 (1983); **B226**, 405 (1983); K. Ishikawa et al., *Phys. Lett.* **116B**, 429 (1982); *Z. Phys.* **C21**, 167 (1983).
[159] C. E. Carlson et al., *Phys. Rev.* **D27**, 1556 (1983); **D28**, 2895 (1983); T. Barnes et al., *Phys. Lett.* **110B**, 159 (1982); *Nucl. Phys.* **B198**, 380 (1982); J. F. Donoghue et al., *Phys. Lett.* **99B**, 416 (1981).
[160] N. V. Krasnikov et al., *Z. Phys.* **C19**, 301 (1983); P. Pascual, R. Tarrach, *Phys. Lett.* **113B**, 495 (1982); S. Narison, *Phys. Lett.* **125B**, 501 (1983); *Z. Phys.* **C26**, 209 (1984); V. A. Novikov et al., *Nucl. Phys.* **B191**, 301 (1981).
[161] D. Scharre et al., *Phys. Lett.* **97B**, 329 (1980).
[162] S. Chung et al., *Phys. Rev. Lett.* **55**, 779 (1985).
[163] A. Ando et al., KEK preprint 86-8, 1986.
[164] S. Meshkov, W. F. Palmer, S. S. Pinsky, preprint DOE/ER/01545-382, 1986.
[165] H. Aihara et al., *Phys. Rev. Lett.* **57**, 51 (1986).
[166] C. Edwards et al., *Phys. Rev. Lett.* **49**, 259 (1982).
[167] J. E. Augustin et al., contributed paper to the International Conference on High Energy Physics, Bari, July 1985 and Orsay preprint LAL/85-27.
[168] M. Chanowitz, *Phys. Lett.* **164B**, 379 (1985).
[169] M. Frank, P. J. O'Donnell, Ref. [109]; C. Rosenzweig et al., *Phys. Rev.* **D24**, 2545 (1981);

N. N. Achasov, G. N. Schestakov, *Phys. Lett.* **156B**, 434 (1985); H. E. Haber, J. Perrier, *Phys. Rev.* **D32**, 2961 (1985).

[170] S. Narison, N. Pak, N. Paver, *Phys. Lett.* **147B**, 162 (1984).

[171] H. J. Lipkin, at Fermilab Workshop on Antimatter Physics at Low Energy and Argonne preprint ANL-HEP-CP-86-29, 1986.

[172] H. J. Lipkin, *Phys. Lett.* **171B**, 298 (1986).

[173] C. Edwards et al., *Phys. Rev. Lett.* **48**, 458 (1982).

[174] J. M. Cornwall, A. Soni, *Phys. Lett.* **120B**, 431 (1983); C. E. Carlson et al., T. Barnes et al., J. F. Donoghue et al., in Ref. [159]; V. A. Novikov et al., in Ref. [160]; K. Johnson, C. B. Thorn, *Phys. Rev.* **D13**, 1934 (1976); R. L. Jaffe, K. Johnson, *Phys. Lett.* **60B**, 201 (1976).

[175] B.-A. Li et al., Stony Brook preprint ITP-SB-86-29, 1986.

[176] M. Althoff et al., *Phys. Lett.* **121B**, 216 (1983).

[177] F. Caruso, E. Pedrazi, Turin preprint DFTT-8/86, 1986.

[178] M. Althoff et al., *Z. Phys.* **C29**, 189 (1985).

[179] J. Turnau, *Z. Phys.* **C25**, 299 (1984).

[180] F. de Viron, J. Govaerts, *Phys. Rev. Lett.* **53**, 2207 (1984); J. Govaerts et al., *Nucl. Phys.* **B248**, 1 (1984).

[181] J. Latorre et al., *Phys. Lett.* **147B**, 171 (1984); J. Latorre et al., Trieste preprint IC/85/299.

[182] J. I. Balitsky et al., *Phys. Lett.* **112B**, 71 (1982).

[183] T. Barnes et al., *Nucl. Phys.* **B224**, 241 (1983).

[184] M. Chanowitz, S. Sharpe, *Nucl. Phys.* **B222**, 221 (1983).

[185] M. Tanimoto, *Phys. Rev.* **D27**, 2648 (1983).

[186] N. Isgur et al., *Phys. Rev. Lett.* **54**, 869 (1985).

[187] J. M. Cornwall, S. F. Tuan, *Phys. Lett.* **136B**, 110 (1984).